ELSEVIER

Contents lists available at ScienceDirect

# Forest Ecology and Management

journal homepage: www.elsevier.com/locate/foreco





# The shadeshed: A lidar-based variable width shade buffer and riparian core for headwater streams

Douglas J. Martin <sup>a,\*</sup> , Bernard Romey <sup>b</sup>, Alice A. Shelly <sup>c</sup>, Kevin Andras <sup>d</sup>

- <sup>a</sup> Martin Environmental LLC, Seattle, WA, USA
- <sup>b</sup> Romey Riverscape Science, Longview, WA, USA
- <sup>c</sup> Kleinschmidt Associates, Redmond, WA, USA
- d TerrainWorks, Mt. Shasta, CA, USA

#### ARTICLE INFO

Keywords:
Variable-width buffer
Lidar-light penetration index
Stream shade
Stream temperature
Headwaters
Riparian management

# ABSTRACT

The high density of headwater streams within working forests poses challenges to forest managers seeking to maintain riparian ecosystem functions while balancing forest production. Buffer guidelines vary among jurisdictions, stream size, and land ownership, but most incorporate a fixed-width buffer structure that is assumed protective of ecosystem functions and administratively simple to implement. However, prescriptive one-size-fitsall buffer rules often fail to achieve the intended goals when uniformly applied across spatially diverse and temporally dynamic watersheds and stream systems. Therefore, new approaches are needed that address spatial variability and focus on riparian ecological functions not only to improve effectiveness of riparian management but increase certainty of outcomes. To address these knowledge gaps, we experimentally tested the effectiveness of a variable-width-shade buffer (VWSB) to provide effective shade (ES), maintain stream temperature, and ontimize riparian tree retention across nineteen headwater streams in Washington, USA. We employed GIS to delineate the riparian forest area that obstructs midday direct beam solar radiation (i.e., shadeshed zone) and used the shadeshed zone to guide the location and size of VWSBs. We used Lidar and the Light Penetration Index (LPI) to estimate effective shade retained within the shadeshed zone and validated the accuracy of LPI with hemispherical photography to produce continuous and accurate estimates of effective shade over streams. We estimated pre- post-harvest changes in effective shade and water temperature to evaluate the relative effectiveness of the VWSB as compared to the fixed-width discontinuous forest practice buffer (FPB) specified under current Washington State (USA) Forest Practice rules. Our results demonstrated that shade losses at VWSB units were generally similar to or less than those observed at FPB units and that post-harvest shade is maximized when the percentage of shadeshed zone area buffered is maximized. Also, the VWSB proved to be more efficient than the FPB for minimizing riparian timber retention to maintain ES and improve buffer performance across a wide range of buffer sizes. Water temperature responses to buffer treatments were highly variable and no difference was discernible in the mean summertime seven-day moving average of daily maximum stream temperature between treatments. Exploratory analyses suggested a temperature-shade relationship that varied depending on the amount of shrub cover and the percentage of study reach length with surface flow, and potentially groundwater inflow in combination with shade loss. The collective findings demonstrated that the VWSB and shadeshed concepts provide an innovative and effective new approach for designing variable width shade buffers in complex topography.

#### 1. Introduction

The high density of headwater streams within working forests poses challenges to forest managers seeking to maintain riparian ecosystem functions while balancing forest production (Jayasuriya et al., 2022).

Buffer guidelines vary among jurisdictions, stream size, and land ownership, but most incorporate a fixed-width buffer structure that is assumed protective of ecosystem functions and administratively simple to implement (Kuglerová et al., 2020; Richardson et al., 2012). However, prescriptive one-size-fits-all buffer rules often fail to achieve the

E-mail address: doug@martinenv.com (D.J. Martin).

<sup>\*</sup> Corresponding author.

intended goals when uniformly applied across spatially diverse and temporally dynamic watersheds and stream systems (Reeves et al., 2022). The emphasis on structural outcomes (e.g., specific buffer width and length) restricts management options for maintaining riparian ecosystem functions (e.g., shade) and optimization of buffer contributions to beneficial uses (Kuglerová et al., 2014; Newton and Ice, 2015). In the Pacific Northwest USA (PNW-USA), the effectiveness of buffering fishless headwater streams is a debatable issue given current management schemes are neither economically nor ecologically optimal. Recent studies suggest the effectiveness of contemporary forest management practices to maintain water temperature in headwater streams is highly variable and poorly related to riparian canopy cover (Braun et al., 2025; Ehinger et al., 2021; McIntyre et al., 2021; McIntyre et al., 2018; Miralha et al., 2024). In an evidence-based review of thirteen studies of buffer effectiveness to maintain water temperature, Martin et al. (2021) found that the relative effectiveness of most uniformly implemented prescriptive treatments in the PNW-USA varied widely, and that buffer effectiveness was associated weakly with various prescriptive components (e.g., fixed-width, length, patch-buffer). Guidelines for buffering headwater streams in complex topography have been absent, and few studies have tested the effectiveness of riparian treatments tailored to site-specific conditions (Martin et al., 2021; Richardson et al., 2012). Therefore, new approaches are needed that address spatial variability and focus on riparian ecological functions not only to improve effectiveness of riparian management but increase certainty of outcomes.

Researchers have recommended alternative buffer schemes to improve buffer performance and reduce uncertainty of ecological outcomes in topographically complex landscapes (Kuglerová et al., 2014; Martin et al., 2021; Olson et al., 2022; Richardson et al., 2012). To achieve management goals, increasing interest exists in using variable width/retention harvest practices to maintain and/or to enhance riparian ecological functions and facilitate efficient utilization of forest resources (Hasselquist et al., 2021; Ilhardt et al., 2000; Kreutzweiser et al., 2012; Kuglerová et al., 2014). Variable retention harvest is a silvicultural alternative to clearcutting that retains key elements of the existing stand (e.g., snags, mature overstory, down wood) to promote structural diversity and biodiversity in managed forests (Franklin et al. 1997; Franklin and Donato, 2020; Gustafsson et al., 2012). Variable retention thinning of riparian stands in conjunction with upland variable retention harvest has been implemented in British Columbia, Canada to promote biodiversity and mitigate the impacts of clearcutting (Griffith and Kiffney, 2022; Rex et al., 2012). Similarly, variable retention harvest is being implemented as an active riparian management approach to increase light, minimize temperature response, and accelerate development of late-successional conditions in second-growth riparian stands of Northern California USA (Miralha et al., 2024; Roon et al.,

In Washington and Oregon USA, buffer guidelines for headwater streams include provisions for alternate plans (Oregon Dept of Forestry, 2024; Washington, 2005) that allow landowners to implement alternative management schemes if they can provide protection for public resources at least equal in overall effectiveness to the protection provided by the Forest Practices Act and rules (Washington, 2023). Approval of alternate plans is based on showing the potential impacts of a proposed harvest on the level of riparian functions. However, the latter can be difficult, particularly for shade, because labor intensive site-specific surveys and modeling are required to predict post-harvest shade (Boyd and Kasper, 2003). Even though a proposal may be worth the effort, alternate plans are implemented infrequently because of uncertainty about outcomes and lack of experiments to test the efficacy of alternative management schemes (Martin et al., 2021; Richardson et al., 2012).

Retaining riparian vegetation to block direct solar radiation along the sun's pathway across the sky (i.e., effective shade) (Allen and Dent, 2001; Teti and Pike, 2005) has long been advocated as the most effective approach for maintaining water temperature in streams (Beschta et al., 1987; Brazier and Brown, 1973a; Brazier and Brown, 1973b; Johnson,

2004). Direct-beam solar radiation on the water's surface is the dominant source of heat energy that may be absorbed by the water column and streambed (Brown, 1969; Johnson, 2004). Heat absorption is greatest during mid-day when the solar angle of incidence is high (e.g.,  $>40^{\circ}$ ) and most direct-beam radiation is not reflected by the surface albedo (Beschta and Weatherred, 1984; Boyd and Kasper, 2003). Based on Brown's (Brown, 1969) findings, Brazier and Brown (Brazier and Brown, 1973b) developed a densiometer to measure mid-day riparian canopy density along the solar path for a given date (called angular canopy density) and demonstrated a strong relationship between angular canopy density and solar insolation. They proposed that buffer strip designs based on angular canopy density could provide adequate temperature control and optimize the utilization of timber resources. Similarly, Beschta et al. (Beschta et al., 1987) showed that angular canopy density measurements taken during the mid-day period (between 10 a.m. and 2 p.m. in mid to late summer) provide a direct estimate of the shading effects of streamside vegetation. Cafferata (Cafferata, 1990) demonstrated a method for designing buffers by identifying the shade producing areas of riparian stands using a solar pathfinder which can provide accurate and repeatable estimates of solar insolation along the solar path. Similarly, Teti (2001) developed the spherical angular canopy densiometer to directly measure the mid-day effective shade and demonstrated that the angular canopy density measurements are highly comparable to estimates from hemispherical photography (Teti and Pike, 2005). Despite this body of information supporting function-based alternatives (e.g., effective shade buffers), prescriptive fixed-width buffers are the default prescription in the PNW-USA (Richardson et al., 2012).

Here, we investigated the effectiveness of a lidar-based approach for designing variable-width-shade buffers (VWSBs) to provide effective shade in headwater streams. We experimentally tested the operational application of the VWSB design at nineteen locations in western Washington USA and used a weight-of-evidence approach to assess treatment response. Our study objectives were to: 1) use lidar to design variable-width-shade buffers, 2) evaluate the effectiveness of VWSBs to: provide effective shade, minimize changes in stream temperature and optimize timber utilization for riparian buffers, 3) compare the effectiveness of VWSB to a fixed-width buffer 4) evaluate factors potentially influencing VWSB effectiveness, and 5) evaluate the accuracy of lidar for estimating ES over streams.

#### 2. Methods

# 2.1. Study area

We implemented the study in first- and second-order non-fishbearing spatially intermittent headwater (Type Np) streams of western Washington, USA (Fig. 1). The forest practice rules define Type Np waters as perennial streams that do not dry out at any time of the year under normal rainfall and include the intermittent dry portions of the perennial channel below the uppermost point of perennial flow (Washington, 2005). The study region is characterized by highly dissected terrain with steep gradient headwater drainages underlain by glacial till and outwash terrain in the north Cascade/Olympic regions and softer, more eroded sedimentary geology in the southwestern coastal region. The climate is maritime with cool, wet winters and mild dry summers. All study streams were located within intensively managed industrial forest lands with harvestable age (typically 35 – 50 years) conifer stands (mean canopy height of 25 m and mean basal area of 45 m<sup>2</sup>/ha) dominated by Douglas-fir (Pseudotsuga menzeisii) and western hemlock (Tsuga heterophylla). Riparian areas often include a mix of conifer and hardwoods dominated by red alder (Alnus rubra).

Private industrial forestland owners (i.e., members of the Washington Forest Protection Association; WFPA) provided the study units. We asked forestland owners to identify harvest units on non-fish perennial streams that were not disturbed by recent debris-torrents and that could

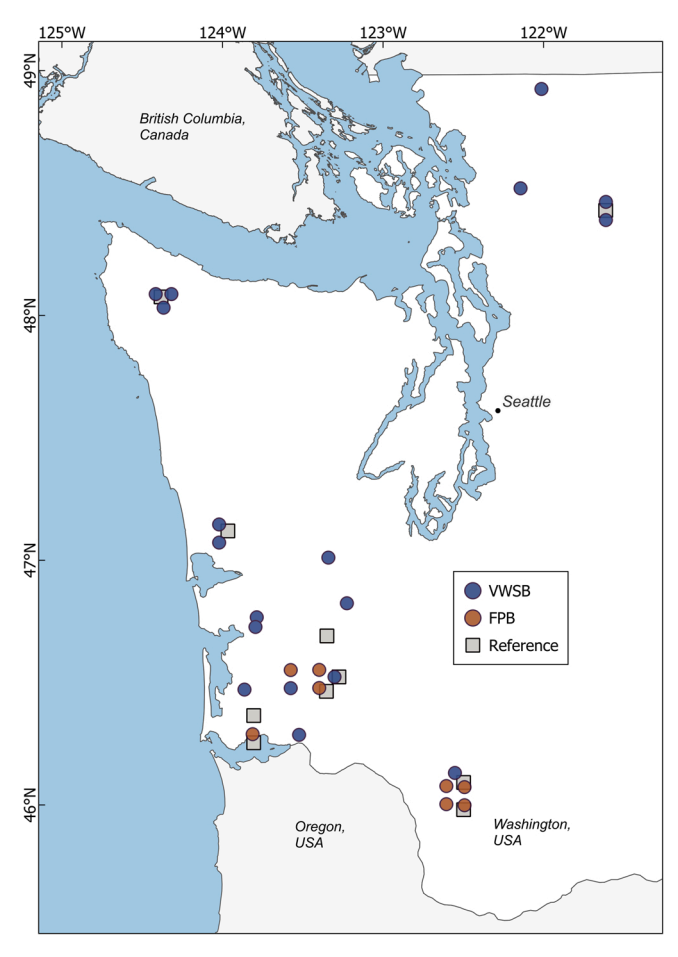


Fig. 1. Locations of VWSB and FPB treatment and reference study units in Western Washington, USA.

be harvested within a schedule to facilitate pre- and post-harvest monitoring. Office reviews of timber harvest plans identified 27 harvest units that were initially planned to have the standard fixed-width discontinuous patch-buffers<sup>1</sup> (hereafter referred to as Forest Practice Buffer, FPB) as specified under current Washington State Forest Practice rules (Washington, 2005). A subset of units (n = 20) was selected by the landowners for the VWSB treatment, and the remainder (7 units) were designated to receive the standard FPB. The application of treatments was not random because each company decided where to implement the VWSB treatments based on considerations for site logistics, coordination with adjacent harvests, and time required for permitting alternate harvest plans. Also, each company identified one or more reference basins (9 total) within the geographic vicinity of the treated study basins and where no timber harvest would occur during the study period. The final set of VWSB study units were geographically widespread and included a wide range of valley orientations, channel gradients, and bankfull widths (BFW) typical of the population of non-fish perennial headwater streams on industrial forest lands of western Washington (Table 1). We note that one site initially designated for a VWSB (HJohn) had to be changed to a wider buffer (F-FPB) treatment because fish were observed just prior to harvest. This site was not included in the evaluation of VWSB performance. However, monitoring was continued through post-harvest at HJohn and data from this site were used in the accuracy estimate analysis for lidar ES. Overall, the evaluation of VWSB performance was based on 35 units; 9, 19, and 7 classified as Reference, VWSB, and FPB units, respectively (Table 1). Most units in this study were harvested during fall-winter 2021 with pre- and post-harvest data collection during 2020–2021 and 2022–2023, respectively. Five units: SHuck1, 2,3, SAllen, and SCap were harvested during fall 2020, with pre- and post-harvest data collection in summer 2020 and 2021–2022, respectively.

#### 2.2. Modeling subcanopy solar insolation

We used the lidar-Light Penetration Index (LPI) to model subcanopy solar insolation (Fig. 2) (Bode et al., 2014; Richardson et al., 2019). The LPI is a proxy for assessing the probability that direct beam radiation will penetrate vegetation and hit the ground (Bode et al., 2014). Lidar three-dimensional point cloud datasets (Appendix Table A1) were obtained from the Washington Lidar Portal (Washington, 2018) for the pre-harvest analyses and from a contracted acquisition for post-harvest analyses. NetMap (Benda et al., 2007) was used to generate synthetic stream networks from the lidar digital terrain model (0.91 m cell size) and vertices (i.e., point where two lines intersect) were placed at every crossed digital terrain model cell. Subcanopy solar insolation (Wh/m<sup>2</sup>) was modeled with the LPI-based approach where insolation is computed from the product of LPI (ratio of ground returns to total returns) and bare-earth radiation. FUSION software (McGaughey, 2021) was used to extract ground returns (i.e., all points falling to within 1.83 m of bare-earth) from the point-cloud. Bare-earth radiation (total daily direct and diffuse) was derived from the ArcGIS solar radiation tool using default values (diffuse solar radiation proportion = 0.3, atmospheric transmissivity = 0.5) and a total solar irradiance value of 1360.8  $\pm$  0.5 W/m2 (Kopp, 2016; Kopp and Lean, 2011). Effective shade was computed as the ratio of the difference between solar radiation above and below canopy, to solar radiation above the canopy (Boyd and Kasper, 2003). The ES calculation incorporated topographic shading because solar radiation above (SRA) stream was derived from bare-earth radiation (Fig. 2). Bare-earth radiation varied along the stream channel depending on the presence of steep topography (e.g., narrow valleys, steep unstable slopes) that may obstruct direct radiation over the stream. Therefore, estimates of bare-earth radiation were used to assess the potential influence of topographic shading on effective shade.

The LPI at any point on the stream surface is determined by shade from neighboring vegetation that obstructs direct beam solar radiation along the solar path. Therefore, we applied a neighborhood analysis to account for shading caused by the local riparian timber stand. For this study, the area of riparian trees obstructing daily direct beam solar radiation at a single point was referred to as a "shadeshed." The size of the shadeshed varies by location as a function of tree height, stream orientation, and solar altitude which, in turn, varies by time-of-day and time of year as the sun moves across the sky (Fig. 3a). FUSION software was used to create a canopy height model which was used to calculate average tree heights within a 30-m by 30-m rectangular neighborhood located proximally to each stream vertex (i.e., centered east-west and shifted south 25 m to encompass most riparian trees within the solar path). The calculation of average tree heights for each rectangular cell accounted for the variation in the riparian composition along the stream channel. We used the sun path and solar altitude geometry for latitude 47.0° (the approximate midpoint between the northern and southern study units; Fig. 1) on August 1st to compute the size of shadesheds at each vertex for midday periods when high-angle direct-beam radiation is most significant for heating streams (Beschta et al., 1987). This was done for midday periods with two durations: 4 h (i.e., 2 h before to 2 h after solar noon) and 6 h (i.e., 3 h before to 3 h after solar noon). The

<sup>&</sup>lt;sup>1</sup> The Washington Forest Practices rules (Washington, 2005) specify a 15.2-m no-harvest buffer on a minimum of 50 % of the Type Np stream network, including a minimum of 91 m immediately upstream of the outlet to fish-bearing waters. Clear-cut harvest to the edge of the channel is allowed on the remainder of the Type Np stream network, with a 9.1-m wide equipment limitation zone (ELZ) to minimize ground disturbance. Patch-buffers are also required on designated sensitive sites including a 17.1-m radius no-harvest buffer centered on each perennial initiation point, referred to as the uppermost point of perennial flow.

Table 1
Study unit characteristics by treatment category.

Treatment	Unit ID	Basin area (ha)	Valley aspect	Length (m)	BFW avg. (m)	Gradient avg. (%)	Unstable slope
Reference	CRef2	17.9	SW	1119	1.25	14.6	yes
Reference	R147	2.5	NW	258	0.79	16.4	yes
Reference	R592	25.0	SW	788	2.37	31.1	yes
Reference	SHuck1	46.0	NE	597	2.13	24.1	yes
Reference	W428650	31.0	N	863	2.01	29.7	yes
Reference	W445740	21.8	W	997	2.07	28.0	yes
Reference	W474760	9.6	S	565	2.33	47.9	yes
Reference	W92614	5.2	W	433	1.90	22.5	yes
Reference	W93504	16.8	W	961	2.38	15.0	yes
VWSB	HElk	6.1	E	418	0.74	14.5	yes
VWSB	HFinn	6.4	S	415	1.05	18.9	yes
VWSB	HQuig	5.2	SW	274	0.76	19.0	yes
VWSB	HSmith	3.2	NE	284	0.86	12.5	yes
VWSB	PMerry	8.8	SW	197	0.94	9.1	no
VWSB	PValue	8.8	NW	431	1.09	17.3	yes
VWSB	R105S	8.0	S	336	1.06	15.7	no
VWSB	R265N	22.7	N	476	3.06	21.4	no
VWSB	R35East	2.6	SW	218	0.91	18.4	no
VWSB	R35West	1.8	S	187	0.81	20.0	no
VWSB	R580S	7.0	NW	174	1.62	16.5	yes
VWSB	SAllen	456.4	S	484	4.90	8.6	no
VWSB	SCap	240.6	SW	588	3.57	14.2	yes
VWSB	SHuck2	8.5	N	369	1.20	24.5	yes
VWSB	W102908	29.7	NW	944	2.23	21.7	yes
VWSB	W22505	38.2	SE	1835	2.52	19.8	yes
VWSB	W426530	10.6	NE	502	1.76	16.7	yes
VWSB	W428550	5.3	W	356	2.02	34.4	yes
VWSB	W93506	13.9	S	394	1.31	10.9	no
FPB	R580N	17.2	W	233	2.29	17.3	yes
FPB	SHuck3	19.9	NE	379	1.85	32.4	yes
FPB	W127880	6.8	NW	264	1.22	10.7	yes
FPB	W127890	7.6	N	289	1.45	18.1	yes
FPB	W22510	8.4	E	202	2.93	34.2	no
FPB	W426550	4.7	NW	357	2.08	23.5	yes
FPB	W92612	14.7	N	712	2.61	24.2	yes

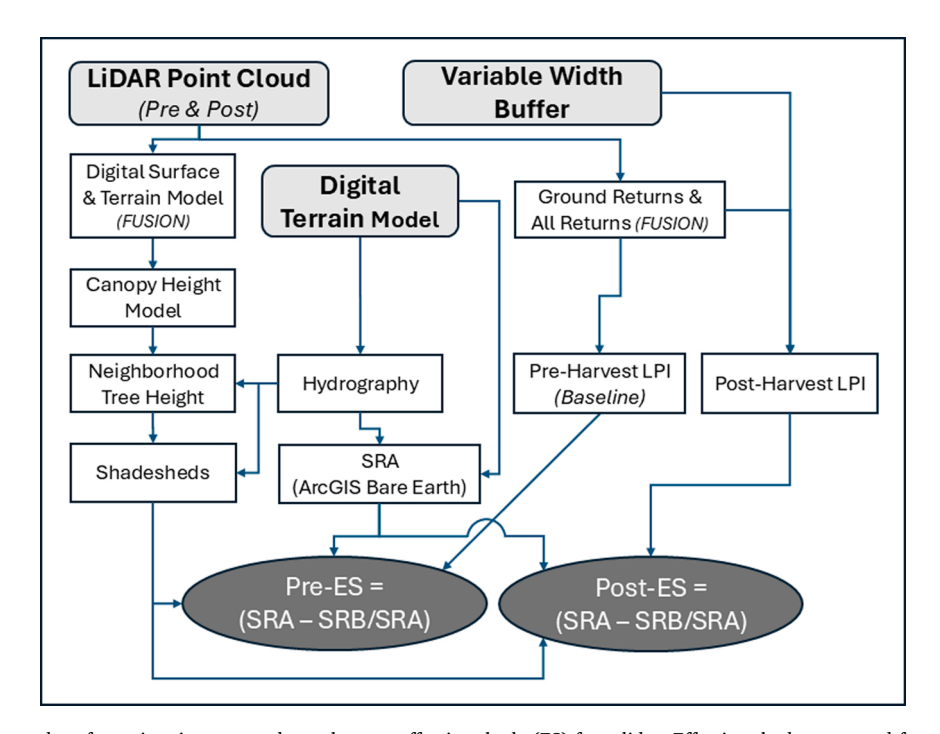


Fig. 2. Flow diagram of procedure for estimating pre- and post-harvest effective shade (ES) from lidar. Effective shade computed from subcanopy solar radiation modeling where: SRA and SRB = total midday solar radiation above and below canopy, respectively.

resulting pie-shaped shadesheds (Fig. 3b) delineated the riparian analysis areas that we used to predict ES. We modeled shade for August 1st because this date represents the mid-summer period when air

temperatures are high, stream flow is low and water temperature is known to be most sensitive to shade loss (Moore et al., 2005; Beschta et al., 1987). Shadesheds were built for each stream vertex ( $\sim 1~\text{m}$ 

# a) Solar Path b) Midday Shadeshed (6-hr) Azimuth: 112° - 246° Vertical Plane Solar Alt.: 43° - 61° Tree Height: 24 m Altitude 25 m ½ arc Solar Azimuth Shadeshed zone (SSZ) Horizontal Plane Boyd & Kasper 2003

Fig. 3. Shadeshed illustration. Panels a) solar path (azimuth, altitude) and tree height factors that influence effective shade, b) 6-hr shadeshed size/shape based on site-specific characteristics, and c) shadeshed zone (SSZ) that is formed by individual pie-shaped midday shadesheds. Shadeshed shadow length (l) = h \*  $\cot(\alpha)$ , where: h = tree height, and  $\alpha$  = solar altitude angle at solar noon. Shadeshed location along the stream channel varies (one side or both sides) in relation to channel orientation.

pixel), and a composite LPI was calculated for each 10-m long stream segment (referred to as a 10-m shadeshed) based on the combined counts of ground returns and total returns for all shadesheds within the segment. A reach-scale LPI was derived from the average LPI for all 10-m shadeshed segments in the study unit and the combined footprint of all shadesheds in the entire reach is hereafter referred to as the shadeshed zone (SSZ; Fig. 3c). We compared LPI estimates of ES (Lidar-ES) to digital hemispherical photography (Hemi-ES) to determine the accuracy of LPI to predict reach-scale ES in a supplemental analysis (Appendix B). The results of this analysis indicated that the 10-m model with 6-hr shadeshed is the best overall predictor for Hemi-ES, with the narrowest 95 % confidence interval over the data range. Given these findings we used the 6-hr Lidar-ES along with Hemi-ES for comparing buffer treatment effectiveness and the 6-hr Lidar-ES for exploring factors influencing buffer treatment outcomes.

# 2.3. Designing variable width buffers

We used the 4-hr shadeshed model for designing the variable width buffers given the forgoing literature about the effectiveness of retaining mid-day shade and because we could not perform the validation analyses of methods (Appendix B) until the end of study when both postharvest lidar and hemi-photo data were available during the same summer. The 4-hr shadeshed models were used to estimate ES for the existing (pre-harvest) and proposed (simulated post-harvest) at each study reach. The estimate of pre-harvest ES provided a baseline for assessing the relative effectiveness of both simulated and actual postharvest ES for the FPB and VWSB units. Pre-harvest ES was based on the shadeshed LPI values for the existing timber stand area within the SSZ (Fig. 4a). The proposed ES for the FPB and VWSB units were simulated for the proposed buffer boundaries that occur within the SSZ and based on the aggregate of pre-harvest LPI values that occurred within the proposed buffer boundaries, and an LPI = 1 for the clearcut (red) areas outside of proposed buffers (Figs. 4b and 4c).

The VWSBs were developed through an iterative process that involved interaction with forest engineers to find an optimal solution for improving buffer performance (i.e., most ES per unit area of tree retention) that would exceed the FPB at the same location. Several proposed VWSB options having different levels of ES were simulated

using the SSZ as a guide. All options included timber retention for the protection of known sensitive areas (e.g., unstable slopes, seeps/springs, tributary junctions) as required by current state forest practice rules, and adjustments to buffer boundaries that were necessary for harvest implementation (e.g., road crossings and yarding corridors). We did not request that landowners maximize the buffering of the SSZ because we were interested in evaluating the effectiveness of the SSZ method with a range of VWSB configurations that varied in size relative to the SSZ (i.e., less or greater than shadeshed width). Harvest unit and buffer-layout plans (obtained from the landowners) were used to simulate ES for the FPB at each VWSB study unit.

# 2.4. Measuring effective shade with digital hemispherical photography

Digital hemispherical photography (Davies-Colley and Payne, 1998; Ringold et al., 2003) was used to estimate ES for each study unit. Hemispherical photos (hemi-phots) were collected during the summer leaf-on period for one to two years preceding and following the timber harvest treatment. Approximately 10 equally spaced photos (maximum spacing of 100 m) were collected along the mainstem channel and some larger tributaries withing the study unit. Annual repeat photos were taken at the same locations except in some cases where a new photo point ( $\pm$  10 m of original) was required because the original point was covered by post-harvest windthrow. Images of the forest canopy were collected at a height of 1.5 m above the stream bed in the center of the channel with a digital camera (Canon 50D or Nikon D40) fitted with a Sigma 4.5-mm f2.8 hemispherical lens. The camera was equipped with a hand-held self-leveling stabilizer attached to a monopod (Arietta, 2022). Camera settings and methods followed the pixel thresholding method developed by Zhao and He (2016) that provides an optimal threshold value for separation of sky and plant pixels. Photos were taken during daylight periods that avoided glare (i.e., early am, late pm, or uniform overcast sky). Hemispherical photos were post-processed and analyzed using Hemisfer software (Schleppi, 2020). The proportion of the total hemisphere blocked by foliage and topography along the solar path (sunrise to sunset) was quantified for August 1st and used for estimating ES at each location. Effective shade is computed from the Hemisfer output as 1- GLI (Global Light Index) where GLI is the proportion of daily solar radiation (direct plus diffuse) under the forest canopy relative to

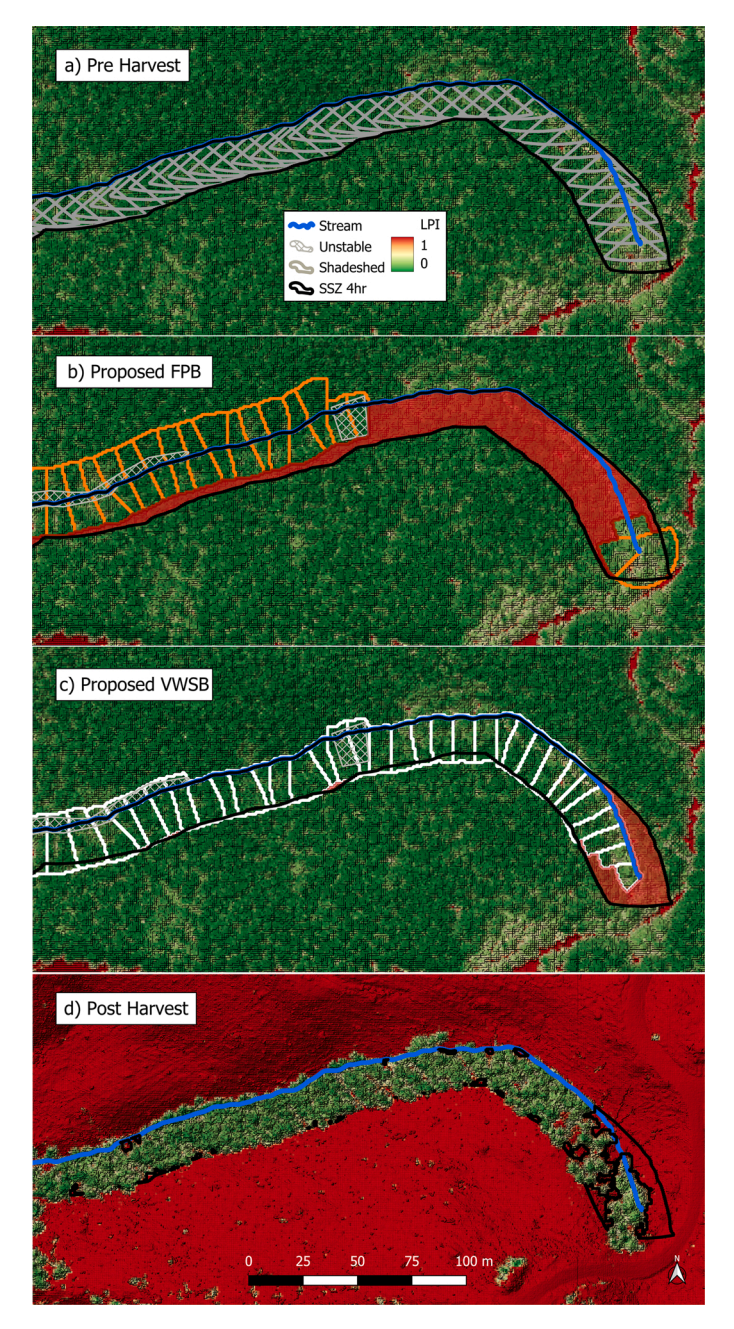


Fig. 4. Illustration of buffer design process using shadeshed and laser penetration index (LPI). Panels show: a) pre-harvest shadeshed zone (SSZ) that is formed by 4-hr midday shadesheds oriented to variations in channel aspect (one-side width ranged 14 – 27 m), b) SSZ and proposed FPB (orange polygons) that includes unstable slope and perennial initiation point buffering, c) SSZ and proposed VWSB (white polygons) that includes unstable slope buffering but excluded perennial initiation point, and d) SSZ and actual post-harvest VWSB with LPI derived from post lidar. The LPI for proposed buffer areas within SSZ boundaries are based on pre-harvest LPI values and LPI = 1 for clearcut (red) areas within the SSZ.

that above.

# 2.5. Temperature Monitoring

We monitored water temperature continuously during the summer season (June 1 to September 30) for one to two years before and after timber harvest at each study unit. Temperature data were recorded at 30-minute intervals with Onset Pendant and Tidbit MX (TidbiT, 2018)

temperature sensors having an accuracy of  $\pm 0.2$  °C. Sensors were checked for drift ( $> \pm 0.5^{\circ}$ C) prior to and following deployment each year using a National Institute of Standards and Technology certified ( $\pm$  $0.2^{\circ}$ C) thermometer. A minimum of two water temperature sensors were located within the lower portion of each study reach. One sensor was placed near the downstream end of reach (i.e., station "zero") and the second one was located 50 m upstream (i.e., station "fifty") of the first sensor. This location scheme provided 1) data from the lowest point in each harvest unit that best represents the combined effects of buffer treatments and timber harvest on stream temperature; 2) two monitoring points to evaluate temperature consistency within the lower non-fish perennial zone of response; and 3) redundancy for cases of a faulty or exposed sensor during low water. A third sensor was located just upstream of the study reach (i.e., station "top") at 14 units with continuous incoming stream flow from unharvested timber upstream. Temperature sensors were secured inside a 5-cm diameter PVC pipe (i.e., to prevent exposure to direct solar radiation) and placed in a pool just above the channel bed and within the thalweg.

For each sensor location, we collated temperature data into datasets for each unit comprising the same period of days for each year. Temperature time series for multiple sensor locations (i.e., top, fifty, zero) within the same unit were plotted together to visually scan for anomalies at individual locations. Daily min, mean, maximum, and diel fluctuations in temperature were graphed and visually reviewed for changes that might indicate dewatering or groundwater influence. Data comparisons were used to determine if the zero, fifty, or both stations were suitable for the analysis of treatment and reference comparisons. Stations with multiple anomalies were removed from the analysis dataset.

#### 2.6. Study unit attributes, channel characteristics and windthrow surveys

Study stream attributes (e.g., gradient, channel orientation) were derived from the NetMap synthetic stream network and buffer characteristics (e.g., buffer area, SSZ area) were measured with QGIS (QGIS, 2024). Channel bankfull width (BFW), shrub cover and surface flow conditions were collected during the summer low-flow period. The BFW was measured (nearest 0.05 m) at each Hemi-photo station. Shrub cover and surface flow were visually estimated (nearest 10 %) within contiguous 10-m long segments along the entire study reach. Shrub cover was only collected during post-harvest period and was defined as understory cover provided by shrubs and small trees (< 4 m tall) hanging over the channel and surface flow was defined as any continuous water surface unbroken by patches of mineral substrate (typically pools or narrow riffles). A survey of windthrow within the post-harvest riparian stands was conducted two years after the buffer treatments. Digital areal photogrammetry was collected with a UAV (Matrice, 2020) equipped with an RTK GPS receiver and flown 90 m above the ground surface with a 90 % front and 85 % side overlap. Individual images were combined into a digital rectified orthophoto in WebODM software (WebODM, 2020) and used to visually count all down trees that intersected the stream.

# 3. Data analysis

# 3.1. Buffer treatment effects on effective shade

The Lidar-ES estimate for each 10-m segment within each study unit was calculated as the ratio of the difference between total midday solar radiation above and below the canopy, to total midday solar radiation above the canopy (Boyd and Kasper, 2003):

$$ES_{ijt} = \frac{SRA_{ijt} - SRB_{ijt}}{SRA_{iit}}, \tag{1}$$

where i= harvest unit, j= 10-m stream segment within harvest unit, t= year (0 for pre=harvest year, 1 for post-harvest year), SRA = the

potential total midday solar radiation above canopy adjusted for julian day, solar altitude, solar azimuth, and site elevation, and SRB = the daily midday solar radiation received at the stream surface.

The Hemi-ES estimate for each photo location was:

$$ES_{ijt} = 1 - GLI_{ijt}, (2)$$

where j = photo location within harvest unit.

For both methods, reach-scale ES was the unit average:

$$ES_{it} = \frac{1}{m} \sum_{i=1}^{m} ES_{ijt}. \tag{3}$$

The change in ES from pre- to post-harvest was estimated for lidar at each 10-m stream segment or hemi-photo location:

$$\Delta ES_{ij} = ES_{ij1} - ES_{ij0},\tag{4}$$

and the average change in shade was the average of these paired differences:

$$\Delta ES_i = \frac{1}{m} \sum_{i=1}^m \Delta ES_{ij} \quad . \tag{5}$$

Because the timing of pre-harvest lidar varied among the study units (reference and treatment), the change in effective shade was adjusted to an annual change (i.e., %/Yr) to account for the time interval between the pre- and post-treatment lidar acquisitions which varied from 3 to 10 years (69 %  $\leq$  5 years) among the study units (Appendix Table A1). Also, the annual  $\Delta ES$  was adjusted relative to the reference units to determine the relative change in shade that can reasonably be attributed to harvest impacts:

$$R\Delta ES_i = \Delta ES_i - \Delta ES_{R_i},\tag{6}$$

where Ri was the reference unit geographically closest to unit i.

The LPI pre-treatment data were based on lidar collected during the leaf-off period (late fall to early spring), while the post-treatment lidar was collected during the summer (leaf-on) period. Therefore, the estimated  $\Delta$ ES may be biased high depending on the quantity of deciduous stands along the study reach that could result in an underestimate of preharvest ES caused by leaf-off conditions. To reduce bias in lidar estimates of  $\Delta$ ES and R $\Delta$ ES, we adjusted the R $\Delta$ ES based on estimates of ES from reference unit riparian segments with conifer dominated stands only, given the assumption that ES at conifer stands during leaf-on and leaf-off are comparable. Therefore, the conifer adjustments resulted in reducing the reference units average  $\Delta ES$  and R $\Delta ES$  from 9.4 % to 5.2 % and from 2.4 % to 1.3 %, respectively based on 6-hr LPI (Appendix Table A2). Also, the riparian stand in one reference unit (R592) was dominated by deciduous trees. Consequently, we replaced this unit with data from an unharvested reach downstream of VWSB unit R580S that was dominated by conifer stands and designated as R580S REF.

During data analysis, we found the designated reference for units in the northeast study group (East of W123 and north of N48; Fig. 1) could not be used to estimate R $\Delta$ ES. Windthrow during the post-harvest study period (associated with an adjacent harvest unit and new road) impacted the riparian canopy causing a negative change in  $\Delta$ ES of -1.7 % and -3.2 % for the 6-hr Lidar-ES and Hemi-ES methods, respectively. Therefore, we used the mean change in ES from all other reference units (i.e., RefMean) to estimate the relative pre-post change in ES because none of the other reference units were close to the northeast group of treatment units.

We used the pre- to post-treatment change in ES  $(\Delta ES_i)$  and relative change in ES  $(R\Delta ES_i)$  from both the hemi-photo and lidar datasets to assess the effectiveness of riparian buffering at each study unit. Shade response at VWSB units were compared individually and collectively with the distribution of responses from the FPB treatments in this study. We also computed a post-treatment buffer performance index (BPI) that

indicated the relative efficiency of a buffer to provide ES given the area of timber retention. The BPI is expressed as the proportion (scale 0–1) of shadeshed zone area with a buffer relative to the total area buffered; and the ratio is weighted by the percentage of effective shade provided by the area of timber retention:

$$BPI = \sqrt{\frac{ES\_pc}{100}} \quad x \quad \frac{SSZ\_area\_ha\left[\frac{SSZ\_bfr\_pc}{100}\right]}{Buff\_ha}$$
 (7)

where BPI = Buffer Performance Index, ES\_pc = Effective Shade (percent), SSZ\_area\_ha = the area inside the SSZ, SSZ\_bfr\_pc = percentage of the SSZ that was buffered, and Buff\_ha = the total post-harvest buffer area. We use the geometric mean to estimate overall buffer performance based on the assumption that each of the riparian variables are nearly equal in importance, only partially compensatory, and that the overall BPI index is weighted by the smallest variable score (Van Horne and Wiens, 1991).

# 3.2. Factors influencing post-treatment effective shade

An exploratory analysis using Spearman correlation, scatter plots, and loess smoothing was conducted to examine potential relationships between post-harvest buffer characteristics and ES. We examined ten post-harvest buffer/stream characteristics that are known to influence buffer shade effectiveness (Boyd and Kasper, 2003; DeWalle, 2010; Grizzel and Wolff, 1998; Rex et al., 2012) including: BFW, buffer area, SSZ area, percentage SSZ area with buffer, length of study reach, percentage of reach length with buffer, portion of study reach flowing east-west, north-south, south, and windthrow frequency (Appendix Table A 3).

#### 3.3. Temperature response

All water temperature analyses were based on the centered 7-day moving average of daily maximum water temperatures (T7DMax). The centered moving average is the arithmetic average of the maximum for the current day and the maximum for three prior and three following days. Before calculating this metric for study and reference units by year, the data were carefully reviewed for evidence of dewatering (sensor exposed to air at low flow) or groundwater influences not reflective of shade influences. The datasets for some units included multiple options for water temperature time series to represent a treatment or reference station (e.g., zero and fifty). The zero station was selected by default unless there was evidence that the zero station was dewatered or clearly driven by groundwater influences. In this case, if the fifty-station appeared to better represent diel and seasonal water temperatures, it was selected (9 of 22 sites) in place of the zero station. If the selection of the zero versus the fifty station was unclear, then both the zero and the fifty locations were included in initial models. In these cases, the treatment station with the largest magnitude of treatment effect relative to the reference station was ultimately selected as it represented the biggest response. For reference units where both the zero and fifty stations were potential reference temperature time series, the reference selection was based on the strength of the pre-harvest linear relationship with the treatment temperatures.

For each reference option, using pre-harvest data only, we fit the model:

$$y_{kt}^{PRE} = \beta_0 + \beta_1 Y ear_k + \beta_2 x_{kt}^{PRE} + \beta_3 Y ear_k x_{kt}^{PRE} + \varepsilon_{kt}$$
(8)

where  $y_{kt} = \text{T7DMax}$  on day t (centered) of year k at the treatment station,  $x_{kt} = \text{T7DMax}$  on day t (centered) of year k at the reference station,  $Year_k = 0$  or 1, included when there are two pre-harvest years,  $\epsilon_{kt} = \varphi_1 \varepsilon_{k(t-1)} + e_{kt}$ ; and  $e_t \sim \text{N}(0, \sigma^2)$ .

The reference station with the lowest value for Akaike's Information

Criterion (corrected for sample size) for this model was used for estimating relative pre- to post- harvest change in temperatures.

Changes in pre- to post-harvest T7DMax water temperatures were estimated for each unit using linear models which assume a linear relationship between T7DMax at the selected reference site and the treatment site and first-order autoregressive (AR[1]) autocorrelation in deviations from this model. Post-harvest impacts included in the model were mean shifts in the T7DMax temperature as well as changes to the relationship between the reference and the treatment site (i.e., interaction effect; shift in slope). To address a potential interaction effect, the overall temperature response was summarized by the pre- to post- harvest estimated change at the mean and the maximum observed T7DMax for the selected reference site (across all sampled years; REFMEAN and REFMAX). This response estimate was included directly in the model by centering the predictor (reference T7DMax) at REFMEAN and REFMAX (two models run). Therefore, the "intercept" term estimated by the model is the REFMEAN or REFMAX intercept rather than a "zero intercept". The changes in the REFMEAN and REFMAX intercepts from pre- to post- harvest (delta response) are the reported treatment effects and are referred to as the  $\Delta$ T7DMavg and  $\Delta$ T7DMmax. All statistical analyses were performed using R statistical software (R-Core-Team).

There were three forms of the linear model used for estimating the treatment effect, based on the number of available years of data in the pre- and post-harvest time periods (maximum two in each), as follows:

1. One year pre- and one-year post-harvest (2 cases): simple comparison of pre year versus post year intercept term in this model:

$$y_{kt} = \beta_0 + \beta_1 \operatorname{Year}_k + \beta_2 (x_{kt} - m) + \beta_3 \operatorname{Year}_k (x_{kt} - m) + \varepsilon_{kt}, \tag{9}$$

where m = max(xkt; REFMAX) or mean(xkt; REFMEAN) and Yeark = 0 for pre year and = 1 for post year. The treatment estimate and 95 % confidence interval were estimated using the gls() and intervals () functions in the nlme package (Pinheiro and Bates, 2000; Pinheiro Bates, 2025).

- 2. Unbalanced years (two pre- and one post- harvest or one pre- and two post-harvest years; 10 cases): with three total years (unbalanced pre-post). Year<sub>k</sub> was treated as a three-level categorical fixed factor. The pre-post shift estimate was found using a linear contrast or generalized linear hypothesis test on Yeark using the function glht() in the package multcomp (Hothorn T, 2008). The approximate 90 % confidence interval was found using the confint() function.
- Two years pre- and two years post-harvest (10 cases). The above model was changed to include a treatment effect with a random effect for year:

$$y_{kt} = \beta_0 + \beta_1 H + \beta_2 (x_{kt} - m) + \beta_3 H(x_{kt} - m) + \tau_k + \varepsilon_{kt},$$
 (10)

where H=0 for pre- and =1 for post-harvest years and  $\tau k$  is the random effect for year k. The estimate for the shift at maximum temperature (H) and confidence intervals were found using the lme() and intervals() functions in the nlme package.

#### 4. Results

#### 4.1. Implementation of VWSB buffer treatments

The implementation of the VWSB treatment resulted in post-harvest buffer areas that were larger (mean = 0.34 ha larger, range 0.05–1.37 ha) than initially proposed at all but one unit (0.22 ha smaller than proposed). Buffering was added during the harvest phase to make site-specific adjustments for sensitive areas (e.g., unstable slopes, seeps, perennial initiation points) and to facilitate harvest implementation. Office plans identified probable sensitive areas and setbacks, but final boundaries and leave areas are often delineated just prior to and during harvest. Also, the proposed VWSB design did not account for harvest permit requirements for some units that deviated from our design (e.g.,

the permit approval required buffering of some perennial initiation point areas that were initially excluded from proposed VWSB design).

# 4.2. Effective shade response to buffer treatments

The reference units had high levels of ES with pre- and post-harvest averages of 95 % and 94 % based on hemi-photos, and 89 % and 94 % based on 6-hr LPI (Appendix Tables A2 and A4). The hemi-phot data indicated that changes in ES were positive and negative (ranged from -3.6--3.2 %) over the pre-post interval (Fig. 5a), whereas the lidar data indicated that ES increased at all reference units (ranged from 0.5 %/yr to 2.2 %/yr) over the pre-post interval (Fig. 5c). Because of the inconsistency between methods, we examined the lidar canopy height data and found that riparian canopy height increased at the reference units by an average of 2.3 m (relative change =0.6 m/yr) over the pre-post-lidar interval (Appendix Table A5).

Bare-earth radiation was highly variable among study units and ranged from 4200 Wh/m $^2$  to 7500 Wh/m $^2$ . A scatterplot of pre-harvest ES versus bare-earth radiation showed no apparent relationship between ES and bare-earth (Appendix Figure A1). Both treatments and the reference groups included units that were influenced by topographic shading as indicated by those with lower bare-earth radiation (< 5500 Wh/m $^2$ ).

We compared the effectiveness of the VWSB and FPB treatments based on the distribution of estimated post-treatment ES and magnitude of change ( $\Delta$ ES, R $\Delta$ ES) as measured by each method. Based on hemiphotos, the range of post-treatment ES results for VWSB was 39–81 %, the median was 68 %, and 14 of 19 units (74 %) had post-treatment ES > 60 % (Appendix Table A6). In comparison, the post-treatment ES results for FPBs ranged from 34 % to 84 %, the median was 53 %, and 2 of 7 units (29 %) had post-treatment ES > 60 %. The changes in ES ( $\Delta$ ES) for VWSB treatments ranged from -12 % to -57 %, with a median of -26 %, and 13 of 19 units (68 %) had  $\Delta$ ES smaller than -30 %, whereas the change ES for the FPB units ranged from -2 % to -60 %, with a median of -42 %, and 2 of 7 (29 %) had  $\Delta$ ES smaller than -30 % (Fig. 5a). The response pattern for relative change in shade (R $\Delta$ ES) was comparable to the pattern for  $\Delta$ ES (Fig. 5b).

The lidar results showed a response pattern similar to hemi-photo findings. The range of post-treatment lidar ES results for VWSB was 46–79 %, the median was 60 %, and 16 of 19 units (84 %) had post-treatment ES > 60 % (Appendix Table A7). In comparison, the post-treatment ES results for FPB ranged from 28 % to 86 %, the median was 50 %, and 2 of 7 (29 %) had post-treatment ES > 60 %. The change in ES for VWSB treatments ranged from 0.7 % to -11.7 %, with a median of -4.4 %, and 14 of 19 (74 %) had  $\Delta$ ES  $\leq$  -6 %/yr, whereas the change in ES for the FPB units ranged from 0.7 to -14.8, with a median of -10.9 %, and 3 of 7 (43 %) had  $\Delta$ ES  $\leq$  -6 %/yr (Fig. 5c). The response pattern for relative change in shade (R $\Delta$ ES) (Fig. 5d) was similar to the pattern for  $\Delta$ ES and showed that most of the FPB units had larger R $\Delta$ ES compared to the VWSB units (e.g., 71 % FPB units and 42 % VWSB units had R $\Delta$ ES > -6 %/yr).

# 4.3. Buffer performance

The buffer performance index (BPI) ranged from 0.51 to 0.78 with a median of 0.68 at the VWSB units and ranged from 0.28 to 0.56 with a median of 0.39 at the FPB units (Fig. 6). Most of the VWSB units (16 of 19) had higher BPI values compared to those at FPB units.

# 4.4. Factors influencing post-treatment effective shade

Exploratory non-parametric correlation analysis suggested positive relationships between post-harvest ES and the percentage of SSZ area buffered and the percentage of reach length buffered (Figs. 7a and 7b). Also, the percentage of SSZ area and percentage of length are correlated with each other. These relationships appeared to be approximately

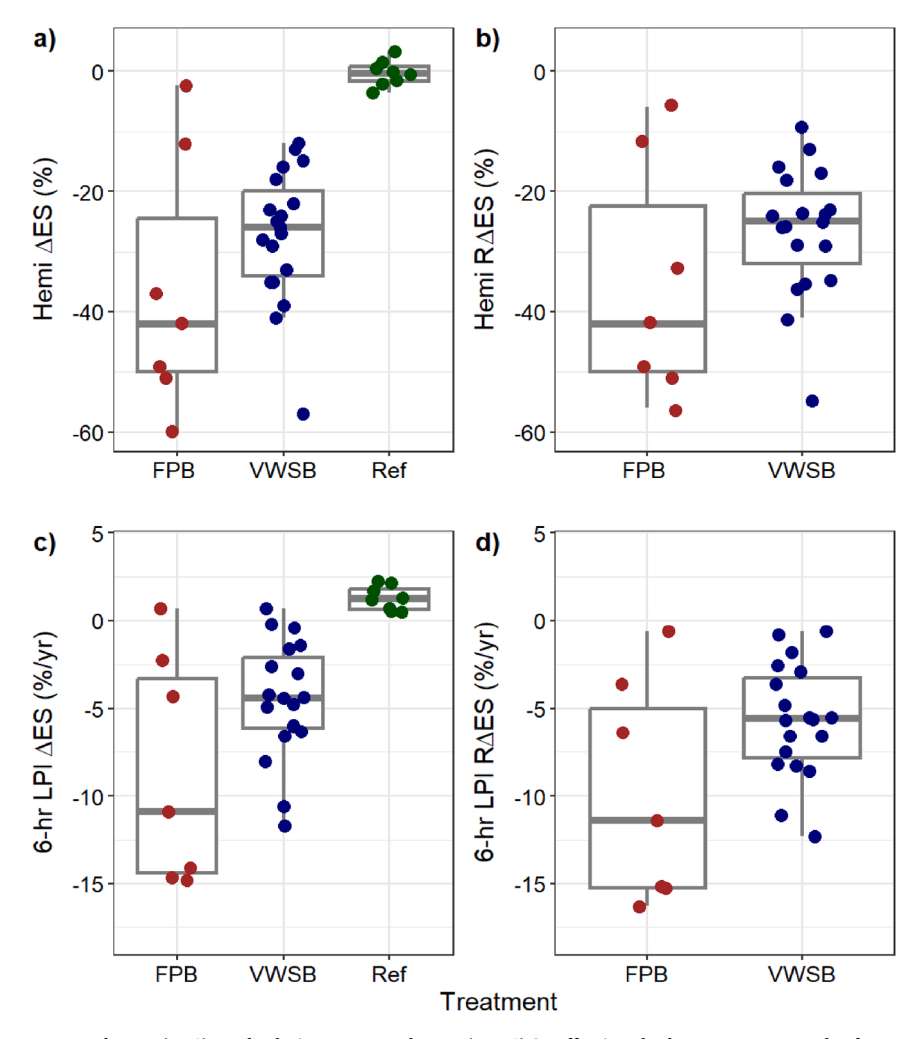
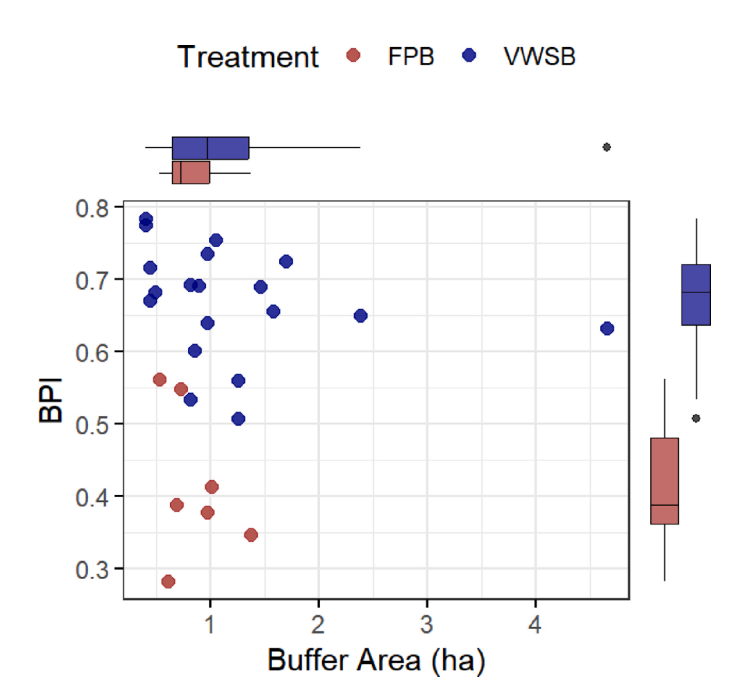


Fig. 5. Pre- and post-harvest average change ( $\Delta$ ES), and relative average change ( $R\Delta$ ES) in effective shade at treatment and reference units. Panels a and b results based on hemispherical photography (Hemi), and panels c and d based on 6-hr laser penetration index (LPI).



**Fig. 6.** Scatter and box plots of post-harvest buffer performance index (BPI) in relation to buffer area by treatment category.

linear with the VWSB treatment units consistently providing more ES compared to the FPB with similar percentages of SSZ area.

The evidence for relationships between ES and other buffer characteristics depended on the buffer treatment. Effective shade was correlated with SSZ area at the FPB units (r = -0.75) but not for the VWSB units (Fig. 7d). Effective shade was related to the proportion of reach length having east-west, north, and south orientations at the FPB units (Figs. 7e, 7f, 7g), but was not related to stream reach orientation at the VWSB units (Appendix Table A8).

Evidence was weak for relationships among ES, buffer area (Fig. 7d), windthrow (Fig. 7h) and channel bankfull width (r=0.24, Appendix Table A8).

# 4.5. Temperature response

The timing of summertime maximum water temperatures differed among years with most peaks occurring during late July through mid-August except for 2021 (Appendix Figure A2). In 2021 the maximum water temperature occurred on June 27th at twenty-two study units and most (89 %) had pre-harvest stands at that time. Eight study units had peak temperatures in mid-August 2021.

Water temperature data from several study units (3 VWSB, I FPB) were not suitable for the analysis because of periodic dewatering at the temperature sensor locations. Therefore, temperature analyses were based on sixteen and six units at the VWSB and FPB treatments, respectively. The water temperature response to buffer treatment was

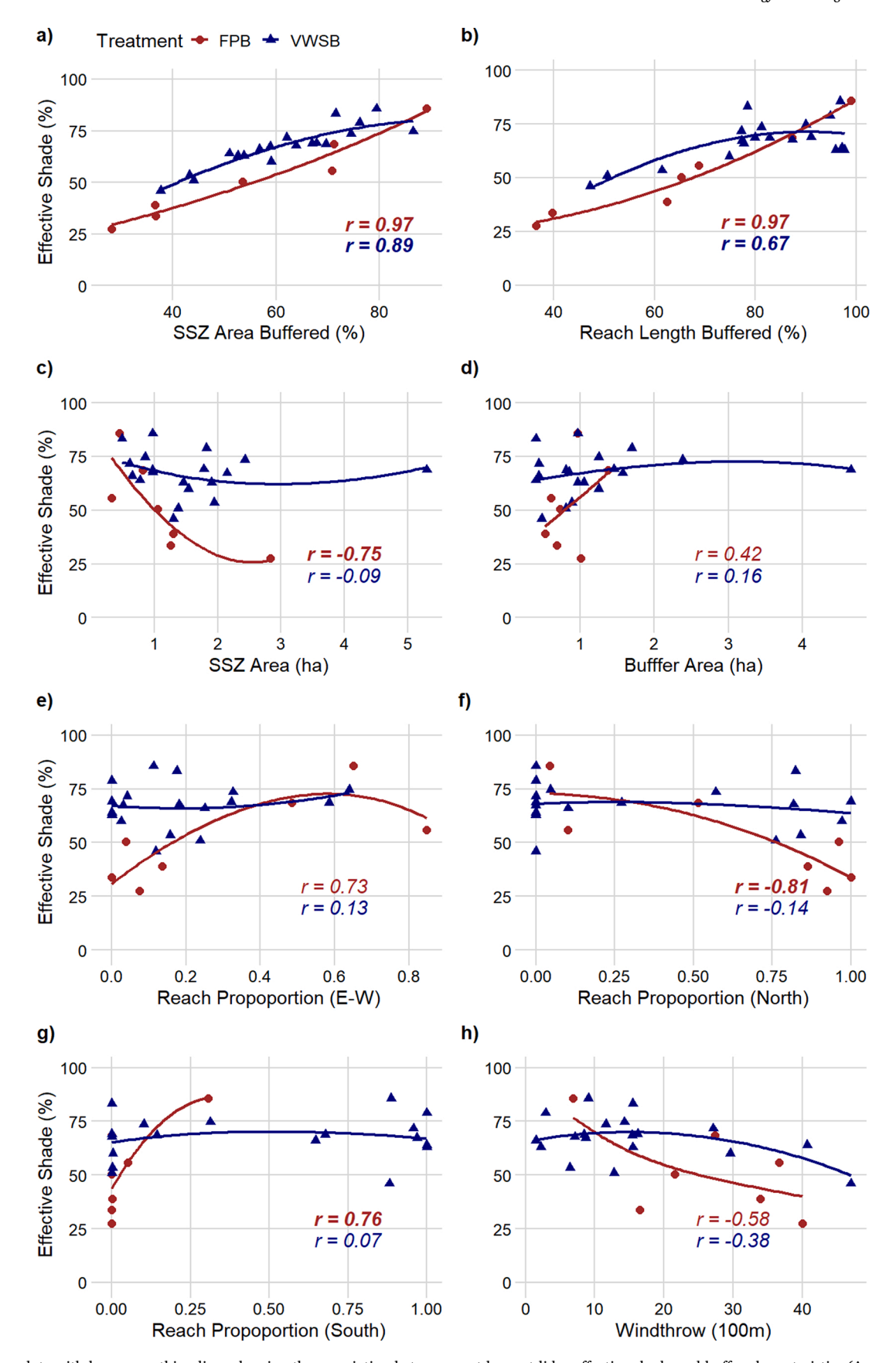


Fig. 7. Scatter plots with loess smoothing lines showing the association between post-harvest lidar effective shade and buffer characteristics (Appendix Table A8). Spearman correlation coefficients with bold values indicate  $p \le 0.05$ .

highly variable both among and within units. Average post-harvest changes at mean reference T7DMax ( $\Delta$ T7DMaxavg) ranged from -0.6 C to 2.1 C for the VWSB treatments and from 0.02 C to 1.4 C for the FPB treatments (Fig. 8, Appendix Table A9). The average post-harvest changes at maximum reference T7DMax ( $\Delta$ T7DMaxmax) were larger and ranged from -1.0 C to 2.4 C and -0.6 C to 2.3 C for the VWSB and FPB treatments, respectively. Uncertainty in these estimates (90 % CI) tended to increase with the magnitude of change except for two units (Helk, PMerry) with small but highly uncertain average pre- to post-changes (i.e., the 90 % CI was greater than 4 C). Given the large 90 % CI among units there is no discernible difference in pre- to post-harvest change in T7DMax between treatments.

Exploratory analyses suggested that the pre- to post-harvest change in T7DMax water temperatures were negatively associated with the average change ( $\Delta ES$ ) and relative average change ( $R\Delta ES$ ) in ES (Table 2). Evidence for a temperature-shade relationship was stronger for the VWSB treatment and for the  $\Delta T7DMax_{avg}$  temperature metric ( $R\Delta ES$ r=-0.64,  $\Delta ES$ r=-0.60). Changes in T7DMax water temperature were weakly correlated with shrub cover, surface flow, and bankfull width.

Given the lack of a strong relationship between changes in effective shade and maximum summer temperatures we further investigated relationships and interactions among the variables in Table 2. using scatter plots of  $\Delta T7DMax_{avg}$  versus R $\Delta ES$  with unit values colored by high and low levels of shrub cover and surface flow (Fig. 9). These plots show that units with the largest changes in relative effective shade generally had the largest changes in maximum summer water temperatures, but no relationship is obvious for small changes in relative effective shade (<7 %). Sites with higher shrub cover tend to have smaller changes in maximum water temperatures (Fig. 9a). Further, there is some indication that units with both small changes in relative shade and higher surface flow, had larger changes in maximum water temperatures

**Table 2**Spearman correlation between the average changes in 7DMax water temperatures versus post-harvest shrub cover, surface flow, bankfull width, and the prepost changes in effective shade. The top and bottom values in each variable row

post changes in effective shade. The top and bottom values in each variable row are VWSP and FPB, respectively. Bold and underlined values indicate  $p \leq 0.01$  and  $p \leq 0.05$ , respectively.

BFW Variable Shrub Surface 6-hr ΔES 6-hr RAES cover (%) flow (%) (m) (%/yr) (%/yr) -0.38 Surface flow -0.54 (%) BFW (m) -0.37 0.60 -0.07 0.21 6-hr ΔES -0.05 0.38 -0.010.32 0.52 0.52 (%/yr) 6-hr R∆ES 0.02 -0.10 0.31 0.28 0.47 (%/vr) 0.56 ΔT7DMax -0.400.19 0.08 -0.60 -0.64 -0.55 0.15 -0.49 -0.34 -0.29ΔT7DMax -0.31 0.12 0.14 -0.48 -0.48 0.30 -0.13 -0.07 -0.51 max

(Fig. 9b). Also, surface flow was positively associated with bankfull width (r = 0.60, Table 2). One unit (SHuck2) with relatively low shade loss similar to others (range -5.0 to -6.0 %/y, Figs. 9a, 9b), moderate windthrow (Appendix A7) and a narrow channel (BFW = 1.2 m) had a noticeable negative temperature response (outlier; -0.6C); suggesting that additional factors may be influencing the magnitude of temperature change.

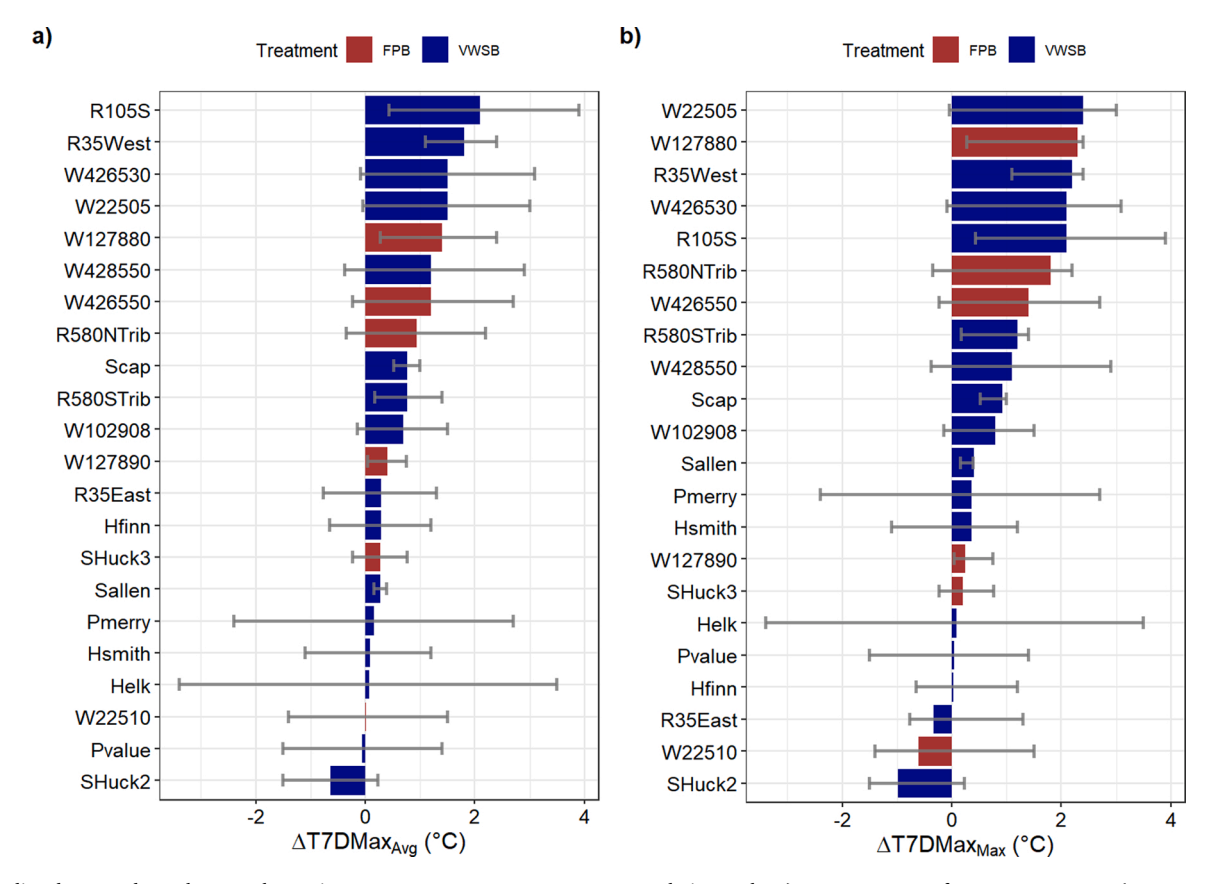


Fig. 8. Predicted pre- and post-harvest change in average 7DMax water temperatures relative to the a) summer mean reference temperature ( $\Delta$ T7DMax $_{avg}$ ) and b) summer maximum reference temperature ( $\Delta$ T7DMax $_{max}$ ). Error bars represent 90 % confidence intervals.

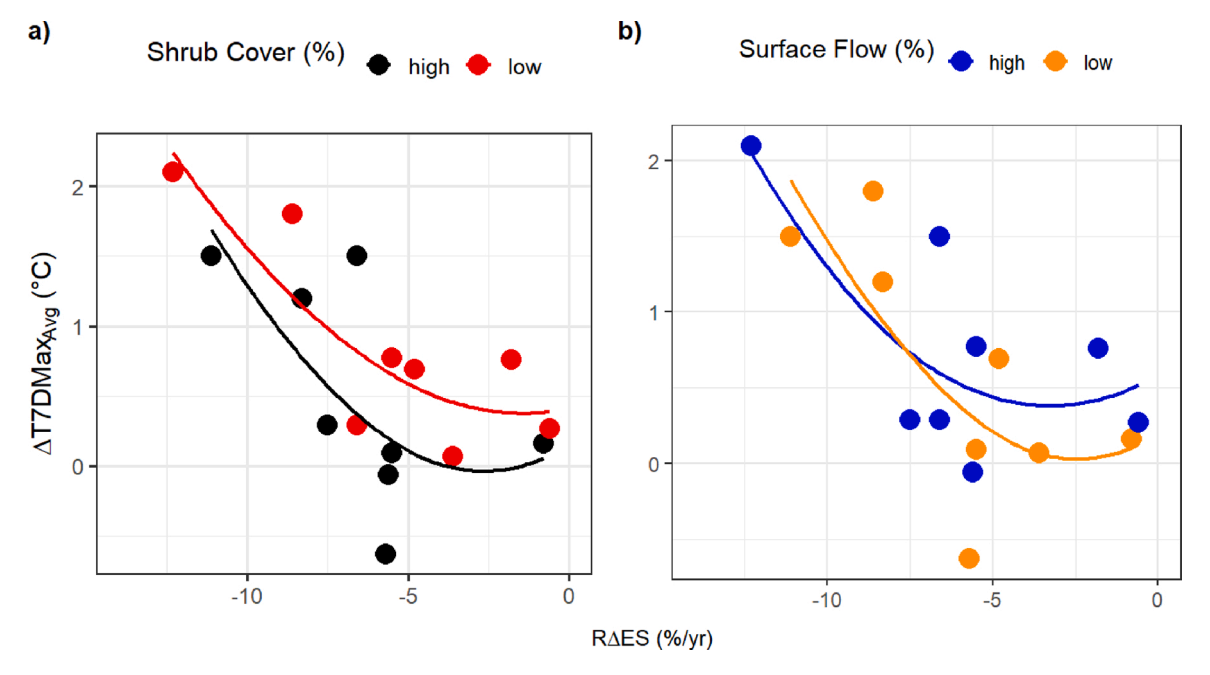


Fig. 9. Scatter plots with loess smoothing line of pre- post-harvest change in 7DMax water temperatures versus the relative average change in effective shade (R $\Delta$ ES) at VWSB units. Panels a) show the temperature response in relation to the percentage of stream reach length with shrub cover, and b) surface flow during summer. We used the median values of 27.3 % and 65.7 % as break points for high and low groupings of shrub cover and surface flow, respectively.

# 5. Discussion

# 5.1. Buffer effectiveness to provide effective shade

Our findings from the hemi-photo and LPI methods of estimating ES demonstrated that shade losses at VWSB units were generally similar to or less than those observed at FPB units. The VWSB treatment produced a gradient of post-harvest ES levels, as planned, resulting in a similar ΔES range between treatments. Results showed that the buffering of sensitive areas (e.g., unstable slopes), especially at some FPB units, increased variability in  $\Delta ES$  responses. Nevertheless, correlation and graphical results suggest that post-harvest shade is maximized when the percentage of the SSZ area buffered is maximized, and VWSB units with similar levels of buffering in the SSZ had consistently higher postharvest effective shade compared to FPB units. The observed relationship between ES and the percentage of reach length buffered also showed how the retention of continuous variable-width timber stands within shadesheds improved buffer effectiveness compared to the discontinuous FPBs. Further, the shadesheds work as proposed because the SSZ size and location were tailored to site-specific conditions (i.e., tree height, channel orientation, solar altitude, topography) that are known to control ES (Beschta et al., 1987; DeWalle, 2010; Sridhar et al., 2004).

Units with the FPB treatment were generally less effective at providing ES than units with the VWSB because the FPB prescriptive layout (i.e., requires patch buffers to be in lower portion of non-fish perennial streams, just upstream of fish-baring waters) does not address how shade is strongly influenced by buffer distribution relative to channel orientation. For example, DeWalle (2010) demonstrated how shading the south side of E-W streams provided proportionately more shade (70 %) compared to buffering the north side (30 %) or buffering both sides of N-S streams. Consequently, the locations of unshaded segments at FPB units can have a disproportionate impact on reach-scale ES depending on channel orientation. For example, our post-harvest exploratory findings showed that ES levels at the FPB units depended upon the locations of patch buffers in channel segments with E-W and N orientations. In contrast, high levels of ES were maintained at VWSB units regardless of channel orientation, demonstrating the effectiveness

of the shadeshed design for buffering shade sensitive areas.

Buffer performance (BPI) for VWSB units was consistently higher than for FPB units and high BPI values were achieved across a wide range of buffer sizes (areas ranged 0.4–4.7 ha). Therefore, the shadeshed buffer configuration of the VWSB provided a more efficient utilization of riparian timber to provide ES compared to the FPB. The high BPI values are a result of retaining high proportions of riparian timber within the SSZ; subsequently maximizing ES while minimizing timber allocation in buffers. The lower BPI at FPB units was due primarily to discontinuous buffering (clearcuts) within the SSZ and the retention of timber in fixed-width patch-buffers outside of the SSZ that provided little or no shade. The retention of buffers on unstable slopes also influenced BPI at both treatments depending on location, in or outside of the SSZ.

BPI is a useful method for comparing the relative performance of different buffer configurations because the index incorporates both timber allocation and ecological function into a single measure of buffer effectiveness. Studies of variable retention and variable width buffer schemes in the Pacific Northwest have focused on buffer effectiveness to control shade/light and water temperature (Foote et al., 2025; Griffith and Kiffney, 2022; Miralha et al., 2024; Rex et al., 2012; Roon et al., 2021). However, we are unaware of any studies that have incorporated evaluations of tradeoffs between ecological benefits (e.g., shade) and the allocation (e.g., cost) of timber resources.

# 5.2. Effective shade and water temperature

High variability in water temperature responses made relationships with effective shade difficult to discern, but the magnitude of water temperature responses was generally associated with the level of shade losses for the VWSB units. The unit with the least shade loss (-0.8 %/yr) had a temperature response of 0.27 C and the unit with the greatest shade loss (-12.5 %/yr) had a temperature response of 2.1 C. For comparison, the corresponding change in ES for these units based on hemiphotos was -13 % and -55 %, respectively. Other studies that evaluated buffer effectiveness with measures of effective shade found that changes in 7DMax were associated with shade loss. For example, Miralha et al. (2024) investigated the effectiveness of variable retention harvest prescriptions in headwaters of northern California and found the

summertime 7DMax temperature increased by 0.4C in association with a 17.5 % reduction in ES and no detectable changes in the 7DMax temperature at sites with ES changes < 1.2 %. Roon et al. (2021) investigated the effects of thinning riparian stands along coastal streams of northern California and found that ES reductions of 23–25 % caused an average increase in 7DMax temperature of 2.5C and ES reductions of less than 5 % resulted in minimal changes in temperature. Shade reductions of 22 % resulted in an average increase in 7DMax temperature of 0.42C. Foote et al. (2025) investigated variable width buffers (varied 3–43 m wide depending on presence of groundwater discharge areas and steep slopes) in western Oregon with average ES reductions of 22 % resulting in an average increase in 7DMax temperature of 0.79C. The latter reported that stream temperature response was associated with shade loss and stream width, and that stream temperature was more sensitive to reductions in shade in smaller (e.g., 2-m wide) streams.

The relationship between post-harvest water temperature response and shade loss in VWSBs was confounded by multiple factors. Our exploratory analyses showed that high variability in the temperatureshade relationship for VWSB units was associated with the amount of shrub cover, surface flow, and potentially other factors in combination with shade loss. For example, the units with higher amounts of postharvest shrub cover (> 27 %) tended to have smaller changes in 7DMax across the observed range of shade loss as compared to units with lower amounts of shrub cover. Although we were unable to assess the pre- to post-harvest changes in shrub cover, we observed rapid growth of residual understory shrubs in canopy gaps during the first summer following treatment and increased shrub cover at many units by the second summer after treatment. Rapid increases (2-3 years after harvesting) in shade from post-harvest deciduous understory has been observed in variable retention buffers of central British Columbia (Rex et al., 2012) and in thinning/riparian patch openings of western Oregon (Anderson and Meleason, 2009). Also, Gravelle and Link (2007) reported that stream temperature changes were minimized by shade from residual understory vegetation following clearcut and partial cut treatments of riparian forests in northern Idaho.

We observed that stream thermal sensitivity increased in relation to the proportion of channel length with surface flow at units with lower levels of shade loss. At these units, surface flow was correlated with channel width and greater post-harvest surface flow (> 66 %) tended to have larger changes in 7DMax as compared to units with similar levels of shade loss but with lesser surface flow. Our observations are limited but are consistent with findings from studies showing that during the summer low-flow period stream segments with surface flow are thermally responsive to shade loss, whereas spatially intermittent segments are unresponsive (Janisch et al., 2012; McIntyre et al., 2021). As the ratio of surface water to groundwater declines, cooler groundwater dominates flow and effectively decouples the correlation between air temperature and stream water response (Braun et al., 2025). We suspect the latter process may explain the post-treatment negative changes in water temperature that we observed at two VWSB units. Other studies of small headwater streams with intermittent flow have documented weak relationships between temperature and shade, and reported that thermal sensitivity can be influenced by multiple geophysical factors (e.g., geology, hydrology, topography; Gomi et al., 2006; Janisch et al., 2012; McIntyre et al., 2021). In contrast, the thermal sensitivity of perennial streams is influenced by stream size (water volumes), in addition to geophysical factors (Boyd and Kasper, 2003; Poole and Berman, 2001), and studies have found that smaller streams are more sensitive to temperature change after shade reduction (Foote et al., 2025; Swartz et al., 2020).

# 5.3. Limitations of findings

Our findings are not based on a spatially representative random sample. However, our VWSB study units were widespread and roughly proportional to the geographic distribution of industrial forest lands in western Washington. The study units included a wide range of valley orientations, channel gradients, and basin sizes that are typical of non-fish headwater streams. Further, our findings represent the variability associated with the operational implementation of the VWSB treatments by five different forestland owners. However, more investigations are needed to validate the effectiveness of the shadeshed concept for designing buffers to maintain ES in a wider range stream sizes and riparian forest conditions.

The accuracy of ES estimates from LPI was influenced by the conifer-deciduous composition of riparian stands and the timing of lidar acquisition. Because pre-harvest effective shade (i.e., derived from lidar during leaf-off season) was underestimated for deciduous portions of riparian stands the estimated post-harvest  $\Delta ES$  was overestimated for some study units. The magnitude of bias is unknown but is likely small given that the average  $\Delta ES$  for all stands (conifer and deciduous) at reference units was 2.4 %/yr and that for conifer-only portions of reference units was 1.3 %/yr; an average difference of 1.1 %/yr. Further, we minimized the potential bias in  $\Delta ES$  at all treatment units by applying an adjustment for the estimates of R $\Delta ES$  based on the conifer-only reference stand  $\Delta ES$ .

To avoid potential bias in estimates of  $\Delta ES$  with lidar, we recommend that LPI be derived from lidar data from the leaf-on season. In the PNW most of the publicly available lidar data has been collected during the leaf-off period to facilitate the production of accurate digital terrain models. Also, the time interval between the year of lidar acquisition and the year for a proposed VWSB should be as short as possible or less than several years, because canopy height and LPI from old lidar data may bias modeled ES estimates for a proposed VWSB design. Acquiring lidar data during leaf-on with drone lidar could provide timely data and more stand detail including understory structure given the higher resolution of drone lidar compared to airborne lidar (Cosenza et al., 2022; Resop et al., 2019).

# 5.4. Management recommendations

#### 5.4.1. Buffer design

Our findings provide strong empirical evidence that the midday shadeshed is an effective tool for guiding the location and size of VWSBs. Further, we showed that post-harvest ES is strongly associated with the proportion of SSZ buffering in VWSB units. This provides evidence that post-harvest changes in water temperature could be lessened with fully buffered shadesheds in streams that are thermally sensitive to shade loss. Both the 4-hr and 6-hr shadeshed are effective models for designing the VWSB depending on channel orientation. For example, at east-west streams the buffer widths for the 4-hr and 6-hr shadesheds are equal because the short radius lengths (i.e., 14 m, Fig. 3b) are identical and the long radius lengths overlap (see east-west portion of Fig. 4a), regardless of shadeshed size. The 6-hr shadeshed is more suitable for buffering north-south streams because the long radius length (i.e., 28 m, Fig. 3b) creates a wider buffer than the 4-hr shadeshed; and would be more effective for intercepting low angle solar radiation during the morning and afternoon.

The shadeshed size for a proposed VWSB should be based on riparian tree heights that are representative of the dominant stand type instead of the local tree height data (30 m X 30 m cell) that was used for our analysis. The latter data incorporated variability in tree heights (due to mixed stands and canopy gaps) which translated to variable shadeshed widths at the 10-m segment scale. The variable-sized shadesheds facilitated accurate estimates of pre-harvest ES but created a jagged and uneven buffer edge that was less suitable for designing the proposed VWSB. Rather, the shadeshed size for a proposed VWSB should be more consistent to facilitate implementation. One simple approach for sizing shadesheds is to use the modal height of riparian stands as was done by (Richardson et al., 2019) for their LPI-based estimate of solar insolation.

Our findings confirmed that August 1st was an effective date for modeling midday ES that corresponded to the seasonal timing of maximum water temperatures during three of our four years of study. The peak summertime temperature on June 27th, 2021, was an abnormality, well outside the historical record for the Pacific Northwest. For example, Seattle WA reached 40°C (104 °F) that day; the city's hottest temperature ever recorded on any day of the year (NASA, 2021). Designing the shadeshed for the mid-summer solar trajectory (August 1st) not only corresponded to the peak temperature period but resulted in a larger shadeshed size than would be the case if based on an earlier date (e.g., higher solar angle at noon on June 21st would reduce shadeshed width by  $\sim\!3$  m).

# 5.4.2. Future implementation

The VWSB is not only well suited for maintaining ES in topographically complex landscapes but could function as the riparian core for adding site-specific buffer management to improve ecological outcomes (e.g., large wood supply, variable light, and erosion reduction). For example, unstable slope and sensitive site buffering (e.g., seeps, springs, groundwater discharge, ecological hotspots) could extend the width of the VWSB or be added to non-shadeshed areas as needed. Each additional area of stand retention should provide a quantifiable ecological function and the priority for inclusion could be based on their relative contribution to ecological outcomes with consideration for optimizing forest resources. Further, the BPI could be used to assess the cumulative buffer performance for any suite of ecological functions and any proposed buffer configuration. Also, buffer planning could be facilitated by new support tools for identifying and mapping channel and hillslope attributes (e.g., erosion potential, landslide hazard; Benda et al., 2007), groundwater inflow areas (Kuglerová et al., 2014), and streamside wetlands (Erdozain et al., 2020; Halabisky et al., 2023).

The variable retention approach accommodates the application of active riparian management schemes to restore complex forest structure, increase understory light, and promote large tree growth in younggrowth riparian stands (Berg, 1995; Kreutzweiser et al., 2012; Martens et al., 2019; Oliver and Hinckley, 1987). Given past (before 1990s) clearcutting along headwater streams, most riparian forests are composed of young stands in the stem exclusion stage (Oliver, 1980) of forest development. Consequently, the natural recovery of desired riparian ecological functions is a multi-decadal to century-scale process (Kaylor and Warren, 2017; Kaylor et al., 2017; Warren et al., 2013). Therefore, the focus on retaining shade, above all else, should not preclude the potential for thinning/partial cuts to increase understory light, promote development of complex multilayered forests (shrubs) and large tree growth (Anderson and Poage, 2014; Roon et al., 2022; Sibley et al., 2012; Swartz et al., 2020). Also, thinning and tipping may be an option to promote large tree growth and jump-start inputs of large wood (Benda et al., 2015). Such treatments could occur in non-shadeshed areas or in shadeshed areas, and their proposed effectiveness to maintain ES could be simulated with LPI as we did in the buffer modeling process.

# 6. Conclusions

Our study of 35 headwater basins in western Washington demonstrated how lidar can be used to: a) design a VWSB to provide ES that is tailored to site-specific conditions in complex topography, b) measure ES continuously along the length of each study reach, and c) experimentally test the effectiveness of the VWSB in comparison to fixed-width discontinuous FPB. We created the shadeshed zone with lidar to delineate the riparian vegetation area that obstructs midday direct-beam solar radiation and showed how the shadeshed zone is an effective method for guiding the location and size of VWSBs. Further, we demonstrated that the Light Penetration Index (LPI) provided an accurate estimate of reach-averaged effective shade and that the best shadeshed model explained 91 % of the variability in daily effective shade. These tools facilitated our buffer effectiveness assessment which indicated that the VWSB minimized shade loss and generally retained

greater ES than the prescriptive FPB. More importantly, the findings suggested that post-harvest ES can be maximized by retaining all stands within the shadeshed zone in VWSB units. Therefore, we are confident that the VWSB and shadeshed concepts are effective given the weight of evidence and that post-harvest changes in water temperature could be lessened with fully buffered shadesheds in streams that are thermally sensitive to shade loss. Furthermore, the VWSB concept is generalizable and provides knowledge that is transferable for developing function-based shade management schemes for all streams. Finally, we propose that riparian management programs shift away from the current structural outcome approach (i.e., prescriptive fixed-width design) to a functional outcome approach tailored to site-specific conditions and eliminating buffer width decisions.

# Funding

This research was funded by the Washington Forest Protection Association.

# CRediT authorship contribution statement

**Douglas J. Martin:** Conceptualization, Writing original draft, Writing and editing, Study design, Analysis. **Bernard Romey:** Writing and editing, Study design, Data collection, Analysis. **Alice A. Shelly:** Analysis. **Kevin Andras:** GIS/Lidar software methodology.

# **Declaration of Competing Interest**

The authors declare the following financial interests/personal relationships which may be considered as potential competing interests: Douglas J. Martin reports financial support and article publishing charges were provided by Washington Forest Protection Association. Douglas J. Martin reports a relationship with Washington Forest Protection Association that includes: consulting or advisory. If there are other authors, they declare that they have no known competing financial interests or personal relationships that could have appeared to influence the work reported in this paper.

# Acknowledgments

We thank the timber companies and forest managers who facilitated implementation of the buffer treatments. Special thanks to timber company technicians (Rayonier, Sierra Pacific, Weyerhaeuser) who assisted with data collection and the statistical support group at Weyerhaeuser for assisting with design of the water temperature statistical analysis. Reviews by A.J. Kroll, Ashley Coble, Jessica Homyack, Jason Walters and peer reviewers greatly improved the manuscript. We thank the Washington Department of Ecology for providing the GIS data for the WDNR study units and the Oregon Department of Environmental Quality for granting permission to include Fig. 3a from (Boyd and Kasper, 2003).

# Appendix A. Supporting information

Supplementary data associated with this article can be found in the online version at <a href="doi:10.1016/j.foreco.2025.123343">doi:10.1016/j.foreco.2025.123343</a>.

#### Data availability

Data will be made available on request.

# References

Allen, M., Dent, L., 2001. Shade conditions over forested streams In the Blue Mountain and coast range georegions of Oregon. ODF Tech. Rep. #13). Retrieved from. (https://www.oregon.gov/odf/Documents/workingforests/monitoring-technical-report -13.pdf).

- Anderson, P.D., Meleason, M.A., 2009. Discerning responses of down wood and understory vegetation abundance to riparian buffer width and thinning treatments: an equivalence-inequivalence approach. Can. J. For. Res. 39 (12), 2470–2485. https://doi.org/10.1139/x09-151.
- Anderson, P.D., Poage, N.J., 2014. The Density Management and Riparian Buffer Study: A large-scale silviculture experiment informing riparian management in the Pacific Northwest, USA. For. Ecol. Manag. 316 (0), 90–99. https://doi.org/10.1016/j. foreco.2013.06.055.
- Arietta, A.Z.A., 2022. Evolutionary Dynamics of Rapid, Microgeographic Adaptation in an Amphibian Metapopulation (Ph.D). Yale University.
- Benda, L., Miller, D., Andras, K., Bigelow, P., Reeves, G., Michael, D., 2007. NetMap: A new tool in support of watershed science and resource management. For. Sci. 53 (2), 206–219. https://doi.org/10.1093/forestscience/53.2.206.
- Benda, L., Litschert, S.E., Reeves, G., Pabst, R., 2015. Thinning and in-stream wood recruitment in riparian second growth forests in coastal Oregon and the use of buffers and tree tipping as mitigation. J. For. Res. 1–16. https://doi.org/10.1007/ s11676-015-0173-2.
- Berg, D.R., 1995. Riparian silvicultural system design and assessment in the Pacific Northwest Cascade Mountains, USA. Ecol. Appl. 5 (1), 87–96. https://doi.org/ 10.2307/1942054
- Beschta, R.L., Weatherred, J., 1984. A computer model for predicting stream temperatures resulting from the management of streamside vegetation. Retrieved Fort Collins Colo. USA. (https://www.bing.com/search?q=A+computer+model+for+predicting+stream+temperatures+resulting+from+the+management+of+streamside+vegetation&form=ANNTH1&refig=4fb6e0aad5764d8392d74996b5bb4457&pc=W011).
- Beschta, R.L., Bilby, R., Brown, G., Hoitby, T., 1987. Stream temperature and aquatic habitat: fisheries and forestry interactions. In: Salo, In.E.O., Cundy, T.W. (Eds.), Streamside Management: Forestry and Fisheries Interactions. University of Washington, Institute of Forest Resources, Seattle, WA, pp. 191–232.
- Bode, C.A., Limm, M.P., Power, M.E., Finlay, J.C., 2014. Subcanopy Solar Radiation model: Predicting solar radiation across a heavily vegetated landscape using LiDAR and GIS solar radiation models. Remote Sens. Environ. 154, 387–397. https://doi. org/10.1016/j.rse.2014.01.028.
- Boyd, M., Kasper, B., 2003. Analytical methods for dynamic open channel heat and mass transfer: Methodology for heat source model Version 7. Oregon Department of Environmental Quality, Salem, OR. Retrieved from. <a href="http://www.deq.state.or.us/wg/IMDIs/tools.htm">http://www.deq.state.or.us/wg/IMDIs/tools.htm</a>).
- Braun, D.C., Cunningham, D.S., Herunter, H.E., Naman, S.M., Martens, A.M., 2025. Long-term trajectories of impacts and recovery of headwater stream temperatures after forest harvest in interior British Columbia. For. Ecol. Manag. 585, 122613. https://doi.org/10.1016/j.foreco.2025.122613.
- Brazier, J.R., & Brown, G.W. (1973a). Buffer strips for stream temperature control (Research paper 15). Retrieved from (https://www.semanticscholar.org/paper/Buffer-strips-for-stream-temperature-control-Brazier-Brown/0609967bf588cf4659ccd74233205dce9552c8b7).
- Brazier, J.R., & Brown, G.W. (1973b). Buffer strips for stream temperature control (Research Paper 15). Retrieved from Corvallis, OR:
- Brown, G.W., 1969. Predicting Temperatures of Small Streams. Water Resour. Res. 5 (1), 68–75. https://doi.org/10.1029/WR005i001p00068.
- Cafferata, P., 1990. Watercourse temperature evaluation guide. California Department of Forestry and Fire Protection, Sacramento, CA. Retrieved from. <a href="https://www.researchgate.net/publication/272090813\_Watercourse\_Temperature\_Evaluation\_Guide">https://www.researchgate.net/publication/272090813\_Watercourse\_Temperature\_Evaluation\_Guide</a>). Cosenza, D.N., Vogel, J., Broadbent, E.N., Silva, C.A., 2022. Silvicultural experiment
- Cosenza, D.N., Vogel, J., Broadbent, E.N., Silva, C.A., 2022. Silvicultural experiment assessment using lidar data collected from an unmanned aerial vehicle. For. Ecol. Manag. 522. 120489. https://doi.org/10.1016/i.foreco.2022.120489.
- Davies-Colley, R.J., Payne, G.W., 1998. Measuring Stream Shade. J. North Am. Benthol. Soc. 17 (2), 250–260. https://doi.org/10.2307/1467966.
- DeWalle, D.R., 2010. Modeling Stream Shade: Riparian Buffer Height and Density as Important as Buffer Width. JAWRA J. Am. Water Resour. Assoc. 46 (2), 323–333. https://doi.org/10.1111/j.1752-1688.2010.00423.x.
- Ehinger, W.J., Estrella, S., Bretherton, W., Schuett-Hames, D., Stewart, G., S, N., 2021. Effectiveness of Forest Practices Buffer Prescriptions on Perennial Non-fish-bearing Streams on Marine Sedimentary Lithologies in Western Washington (Cooperative Monitoring. Eval. Res. Comm. Rep. CMER 2021. 08. 24). Retrieved Olymp. WA (fp. cmer typen soft rock.pdf).
- Erdozain, M., Emilson, C.E., Kreutzweiser, D.P., Kidd, K.A., Mykytczuk, N., Sibley, P.K., 2020. Forest management influences the effects of streamside wet areas on stream ecosystems. Ecol. Appl. 30 (4), e02077. https://doi.org/10.1002/eap.2077.
- Foote, A.W., Sanders, A.M., Coble, A.A., Warren, D.R., 2025. Stream Temperature Response to Riparian Buffer Configurations: A Replicated Experiment Across Oregon's Coast Range. Hydrol. Process. 39 (10), e70278. https://doi.org/10.1002/ hyp.70278.
- Forestry, O.D.O., 2024. For. Pract. Adm. Rules Or. For. Pract. Act. Retrieved from \(\lambda\)ttps://www.oregon.gov/odf/documents/workingforests/fpa-rule-book-2024.pdf).
- Franklin, J.F., Donato, D.C., 2020. Variable retention harvesting in the Douglas-fir region. Ecol. Process. 9 (1), 8. https://doi.org/10.1186/s13717-019-0205-5.
- Franklin, J.F., Berg, D.E., Thornburgh, D.A., Tappeiner, J., 1997. Alternative silvicultural approaches to timber harvest: variable retention harvest systems. In: Kohm, K.A., Franklin, J. (Eds.), Creating a forestry for the 21st Century. Island Press, Washington DC. USA. pp. 111–139.
- Gomi, T., Moore, R.D., Dhakal, A.S., 2006. Headwater stream temperature response to clear-cut harvesting with different riparian treatments, coastal British Columbia, Canada. Water Resour. Res. 42 (8). https://doi.org/10.1029/2005wr004162.

- Gravelle, J.A., Link, T.E., 2007. Influence of Timber Harvesting on Headwater Peak Stream Temperatures in a Northern Idaho Watershed. For. Sci. 53 (2), 189–205. https://doi.org/10.1093/forestscience/53.2.189.
- Griffith, J.E., Kiffney, P.M., 2022. Seasonal and temporal variation in the effects of forest thinning on headwater stream benthic organisms in coastal British Columbia. For. Ecol. Manag. 504, 119801. https://doi.org/10.1016/j.foreco.2021.119801.
- Grizzel, J., Wolff, N., 1998. Occurrence of windthrow in forest buffer strips and its effect on small streams in northwest Washington. Northwest Sci. 72 (3), 214–223. Retrieved from. (https://research.libraries.wsu.edu/xmlui/handle/2376/1210? show=full).
- Gustafsson, L., Baker, S.C., Bauhus, J., Beese, W.J., Brodie, A., Kouki, J., Franklin, J.F., 2012. Retention Forestry to Maintain Multifunctional Forests: A World Perspective. BioScience 62 (7), 633–645. https://doi.org/10.1525/bio.2012.62.7.6.
- Halabisky, M., Miller, D., Stewart, A.J., Yahnke, A., Lorigan, D., Brasel, T., Moskal, L.M., 2023. The Wetland Intrinsic Potential tool: mapping wetland intrinsic potential through machine learning of multi-scale remote sensing proxies of wetland indicators. Hydrol. Earth Syst. Sci. 27 (20), 3687–3699. https://doi.org/10.5194/ hess-27-3687-2023.
- Hasselquist, E.M., Kuglerová, L., Sjögren, J., Hjältén, J., Ring, E., Sponseller, R.A., Laudon, H., 2021. Moving towards multi-layered, mixed-species forests in riparian buffers will enhance their long-term function in boreal landscapes. For. Ecol. Manag. 493, 119254. https://doi.org/10.1016/j.foreco.2021.119254.
- Ilhardt, B.L., Verry, E.S., Palik, B.J., 2000. Defining riparian areas. In: Verry, In.E.S., Hornbeck, J.W., Dolloff, C.A. (Eds.), Riparian Management in Forests of the Continental Eastern United States. Lewis Publishers, Boca Raton, FL, pp. 23–42.
- Janisch, J.E., Wondzell, S.M., Ehinger, W.J., 2012. Headwater stream temperature: Interpreting response after logging, with and without riparian buffers, Washington, USA. For. Ecol. Manag. 270, 302–313. https://doi.org/10.1016/j. foreco.2011.12.035
- Jayasuriya, M.T., Germain, R.H., & Stella, J.C. (2022). Applying the "Goldilocks Rule" to Riparian Buffer Widths for Forested Headwater Streams across the Contiguous U.S. -How Much Is "Just Right"? Forests, 13(9), 1509. Retrieved from (https://www.mdpi. com/1999-4907/13/9/1509).
- Johnson, S.L., 2004. Factors influencing stream temperatures in small streams: substrate effects and a shading experiment. Can. J. Fish. Aquat. Sci. 61 (6), 913–923. https:// doi.org/10.1139/f04-040.
- Kaylor, M.J., Warren, D.R., 2017. Canopy closure after four decades of postlogging riparian forest regeneration reduces cutthroat trout biomass in headwater streams through bottom-up pathways. Can. J. Fish. Aquat. Sci. 75 (4), 513–524. https://doi. org/10.1139/cjfas-2016-0519.
- Kaylor, M.J., Warren, D.R., Kiffney, P.M., 2017. Long-term effects of riparian forest harvest on light in Pacific Northwest (USA) streams. Freshw. Sci. 36 (1), 1–13. https://doi.org/10.1086/690624.
- Kopp, G., 2016. Magnitudes and timescales of total solar irradiance variability. J. Space Weather Space Clim. 6, A30. https://doi.org/10.1051/swsc/2016025.
- Kopp, G., Lean, J.L., 2011. A new, lower value of total solar irradiance: Evidence and climate significance. Geophys. Res. Lett. 38 (1). https://doi.org/10.1029/ 2010GL045777.
- Kreutzweiser, D.P., Sibley, P.K., Richardson, J.S., Gordon, A.M., 2012. Introduction and a theoretical basis for using disturbance by forest management activities to sustain aquatic ecosystems. Freshw. Sci. 31 (1), 224–231. https://doi.org/10.1899/11-114.1.
- Kuglerová, L., Ågren, A., Jansson, R., Laudon, H., 2014. Towards optimizing riparian buffer zones: Ecological and biogeochemical implications for forest management. For. Ecol. Manag. 334, 74–84. https://doi.org/10.1016/j.foreco.2014.08.033.
- Kuglerová, L., Jyväsjärvi, J., Ruffing, C., Muotka, T., Jonsson, A., Andersson, E., Richardson, J.S., 2020. Cutting Edge: A Comparison of Contemporary Practices of Riparian Buffer Retention Around Small Streams in Canada, Finland, and Sweden. Water Resour. Res. 56 (9), e2019WR026381. https://doi.org/10.1029/ 2019WR026381.
- Martens, K.D., Devine, W.D., Minkova, T.V., Foster, A.D., 2019. Stream Conditions after 18 Years of Passive Riparian Restoration in Small Fish-bearing Watersheds. Environ. Manag. 63 (5), 673–690. https://doi.org/10.1007/s00267-019-01146-x.
- Martin, D.J., Kroll, A.J., Knoth, J.L., 2021. An evidence-based review of the effectiveness of riparian buffers to maintain stream temperature and stream-associated amphibian populations in the Pacific Northwest of Canada and the United States. For. Ecol. Manag. 491, 119190. https://doi.org/10.1016/j.foreco.2021.119190.
- Matrice, D. (2020). Retrieved from <a href="https://www.dslrpros.com/pages/thermal-drones-lineup/?utm\_source=bing&utm\_medium=cpc\_perf&utm\_term=www.dslrpros.com&utm\_campaign=590304041&utm\_content=&msclkid=2e307fa4605a1795a03517c43400fb49</a>)
- McGaughey, R.J., 2021. FUSION/LDV Softw. LIDAR data Anal. Vis. 2.51 Edn.Retrieved from (https://research.fs.usda.gov/pnw/products/dataandtools/fusion/ldv-lidar-pr ocessing-and-visualization-software-version-440).
- McIntyre, A.P., Hayes, M.P., Ehinger, W.J., Estrella, S.M., Schuett-Hames, D., & Quinn, T. (2018). Effectiveness of experimental riparian buffers on perennial non-fish-bearing streams on competent lithologies in Western Washington (Cooperative Monitoring, Evaluation and Research Report CMER 18-100). Retrieved from Olympia, WA: (https://www.dnr.wa.gov/publications/fp\_cmer\_typen\_hr\_20201119.pdf).
- McIntyre, A.P., Hayes, M.P., Ehinger, W.J., Estrella, S.M., Schuett-Hames, D., Ojala-Barbour, R., Stewart, G., Quinn, T. (2021). Effectiveness of experimental riparian buffers on perennial non-fish-bearing streams on competent lithologies in western Washington Phase 2 (9 years after harvest). Retrieved from Olympia, WA: (https://www.dnr.wa.gov/publications/fp\_emer\_hr\_phase\_ii\_2022.pdf).

- Miralha, L., Segura, C., Bladon, K.D., 2024. Stream temperature responses to forest harvesting with different riparian buffer prescriptions in northern California, USA. For. Ecol. Manag. 552, 121581. https://doi.org/10.1016/j.foreco.2023.121581.
- Moore, R.D., Sutherland, P., Gomi, T., Dhakal, A., 2005. Thermal regime of a headwater stream within a clear-cut, coastal British Columbia, Canada. Hydrol. Process. 19 (13), 2591–2608. https://doi.org/10.1002/hyp.5733.
- NASA. (2021). Exceptional Heat Hits Pacific Northwest. NASA Earth Observatory.

  Retrieved from (https://earthobservatory.nasa.gov/images/148506/exceptional-he
  at-hits-pacific-northwest#:~:text=Local%20ground%20stations%20in%20nume
  rous,F%20\((44%C2%B0C)\).
- Newton, M., Ice, G., 2015. Regulating riparian forests for aquatic productivity in the Pacific Northwest, USA: addressing a paradox. Environ. Sci. Pollut. Res. 1–9. https://doi.org/10.1007/s11356-015-5814-7.
- Oliver, C.D., 1980. Forest development in North America following major disturbances. For. Ecol. Manag. 3, 153–168. https://doi.org/10.1016/0378-1127(80)90013-4.
- Oliver, C.D., Hinckley, T.M. (Eds.), 1987. Species, stand structure, and silvicultural manipulation patterns for the streamside zone (Contribution No. 57 ed.).. University of Washington, Institute of Forest Resources, Seattle, WA.
- Olson, D., Coble, A., Homyack, J., 2022. Beyond Best Management Practices. In: Danehy, R.J., Dolloff, A.C., Reeves, G.H. (Eds.), Reflections on forest management: Can fish and fiber coexist? Bethesda, MD: American Fisheries Society, pp. 279–326. Pinheiro, J., Bates, D. 2000. Mixed-Effects Models in S and S-PLUS, Springer, New York.
- Pinheiro, J., Bates, D., 2000. Mixed-Effects Models in S and S-PLUS. Springer, New York, USA.
- Pinheiro, J. and Bates, D. (2025). nlme: Linear and Nonlinear Mixed Effects Models. R package version 3.1-167. Retrieved from (https://cran.r-project.org/web/packages/nlme/index.html).
- Poole, G.C., Berman, C.H., 2001. An Ecological Perspective on In-Stream Temperature: Natural Heat Dynamics and Mechanisms of Human-CausedThermal Degradation. Environ. Manag. 27 (6), 787–802. https://doi.org/10.1007/s002670010188.
- QGIS, 2024. QGIS Geographic Information System. Open Source Geospatial Found. Proj. Retrieved from <a href="http://www.qgis.org">http://www.qgis.org</a>.
- R-Core-Team. Retrieved from (https://cran.r-project.org/).
- Reeves, G., Benda, L.E., Levesque, S., Cummins, K.W., Ziemer, R., 2022. Environmental Regulation in Temporally Dynamic and Spatially Variable Watershed Environments: Implications for Forest Management. Pap. Presente Reflect. For. Manag. Can. Fish. Fiber coexist? Seattle WA.
- Resop, J.P., Lehmann, L., Hession, W.C., 2019. Drone Laser Scanning for Modeling Riverscape Topography and Vegetation: Comparison with Traditional Aerial Lidar. Drones 3 (2), 35. https://doi.org/10.3390/drones3020035.
- Rex, J.F., Maloney, D.A., Krauskopf, P.N., Beaudry, P.G., Beaudry, L.J., 2012. Variable-retention riparian harvesting effects on riparian air and water temperature of sub-boreal headwater streams in British Columbia. For. Ecol. Manag. 269 (0), 259–270. https://doi.org/10.1016/j.foreco.2011.12.023.
- Richardson, J.J., Torgersen, C.E., Moskal, L.M., 2019. Lidar-based approaches for estimating solar insolation in heavily forested streams. Hydrol. Earth Syst. Sci. 23 (7), 2813–2822. https://doi.org/10.5194/hess-23-2813-2019.
- Richardson, J.S., Naiman, R.J., Bisson, P.A., 2012. How did fixed-width buffers become standard practice for protecting freshwaters and their riparian areas from forest harvest practices? Freshw. Sci. 31 (1), 232–238. https://doi.org/10.1899/11-031.1.
- Ringold, P.L., Van Sickle, J., Rasar, K., Schacher, J., 2003. Use of hemispheric imagery for estimating stream solar exposure. JAWRA J. Am. Water Resour. Assoc. 39 (6), 1373–1384. https://doi.org/10.1111/j.1752-1688.2003.tb04424.x.

- Roon, D., Dunham, J., Bellmore, J., Olson, D., Harvey, B., 2022. Influence of riparian thinning on trophic pathways supporting stream food webs in forested watersheds. Ecosphere 13. https://doi.org/10.1002/ecs2.4219.
- Roon, D.A., Dunham, J.B., Groom, J.D., 2021. Shade, light, and stream temperature responses to riparian thinning in second-growth redwood forests of northern California. PLOS ONE 16 (2), e0246822. https://doi.org/10.1371/journal. pone.0246822.
- Schleppi, P., 2020. Hemisfer a Softw. Des. Estim. leaf Area Index (LAI) Light Regime hemispherical Photogr. Retrieved from (https://www.schleppi.ch/patrick/hemisfer/index.php).
- Sibley, P.K., Kreutzweiser, D.P., Naylor, B.J., Richardson, J.S., Gordon, A.M., 2012. Emulation of natural disturbance (END) for riparian forest management: synthesis and recommendations. Freshw. Sci. 31 (1), 258–264. https://doi.org/10.1899/11-004.1
- Sridhar, V., Sansone, A.L., LaMarche, J., Dubin, T., Lettenmaier, D.P., 2004. Prediction of stream temperature in forested watersheds. J. Am. Water Resour. Assoc. 40 (1), 197–213. https://doi.org/10.1111/j.1752-1688.2004.tb01019.x.
- Swartz, A., Roon, D., Reiter, M., Warren, D., 2020. Stream temperature responses to experimental riparian canopy gaps along forested headwaters in western Oregon. For. Ecol. Manag. 474, 118354. https://doi.org/10.1016/j.foreco.2020.118354.
- Teti, P.A., 2001. A new instrument for measuring shade provided by overhead vegetation. Williams Lake, B.C. Canada (Extension Note No. 34). (https://www.for.gov.bc.ca/rsi/research/cextnotes/extnot34.htm).
- Teti, P.A., Pike, R.G., 2005. Selecting and testing an instrument for surveying stream shade. BC J. Ecosyst. Manag. 6 (2), 1–16. https://doi.org/10.22230/iem\_2005v6n2a310
- TidbiT. (2018). Retrieved from https://www.testequipmentdepot.com/onset-mx2203-hobo-tidbit-mx-temperature-and-water-temperature-400-ft-data-logger.html? msclkid=9ffb8a1f0f0019303b38e27f5dbe790a&utm\_source=bing&utm\_medium=cpc&utm\_campaign=NONS%20-%20Onset%20HOBO%20-% 20USA&utm term=tidbit%20temperature%20datalogger&utm\_content=MX2203.
- Van Horne, B., & Wiens, J.A. (1991). Forest Bird Habitat Suitability Models and the Development of General Habitat Models. (Fish and Wildlife Research 8). Retrieved from https://apps.dtic.mil/sti/tr/pdf/ADA322800.pdf.
- Warren, D.R., Keeton, W.S., Bechtold, H.A., Rosi-Marshall, E.J., 2013. Comparing streambed light availability and canopy cover in streams with old-growth versus early-mature riparian forests in western Oregon. Aquat. Sci. 75 (4), 547–558. https://doi.org/10.1007/s00027-013-0299-2.
- Washington. (2018). Washington Lidar Portal. Retrieved from https://lidarportal.dnr. wa.gov/.
- Washington, D. o N.R. (2005). Forest Practices Rules Title 222 WAC. Retrieved from https://app.leg.wa.gov/WAC/default.aspx?cite=222.
- Washington, D. o N.R. (2023). Forest Practices Board Manual. Section 21, Guidelines for Alternate Plans. Retrieved from https://dnr.wa.gov/dnr-boards-and-commissions/ forest-practices-board/forest-practices-rules-and-board-manual-guidelines/forestpractices-board-manual.
- WebODM. (2020). Retrieved from https://www.opendronemap.org/webodm/.
- Zhao, K., He, F., 2016. Estimating light environment in forests with a new thresholding method for hemispherical photography. Can. J. For. Res. 46 (9), 1103–1110. https:// doi.org/10.1139/cjfr-2016-0003.